Designing and Prototyping of PCM based Thermal Energy Storage System

Muhammad Yousif

Thesis to obtain the Master of Science Degree in

Energy Engineering and Management

Supervisors: Prof. Rui Pedro da Costa Neto

Prof. Carlos Augusto Santos Silva

Examination Committee

Chairperson: Prof. Luís Filipe Moreira Mendes

Supervisor: Prof. Rui Pedro da Costa Neto

Member of the Committee: Dr. Laura Elena Aelenei

October 2019

Abstract

Phase Changer Materials (PCM) are known to have high heat storage density and low thermal conductivity. In order to validate the use of PCM based Thermal Energy Storage (TES) for district heating purposes, a lab-scale validation site of Latent Heat Thermal Energy Storage (LHTES) was designed and constructed.

The selection of suitable commercially available PCM for the given temperature range is done experimentally using the T-history technique. Two types of heat exchangers (HX) are designed; submerged counter flow spiral tube HX and diffuser based macro-encapsulated HX. The low thermal conductivity of PCM is overcome by complex mechanical structure of the HX. The selection of macro-encapsulation is done numerically using COMSOL Multiphysics 5.4.

The T-history experiments done in this study show that Crodatherm-60 is the best PCM for the given temperature range (46°C-72°C). Submerged spiral type HX is designed to have counter flow and fins, to increase the thermal conductivity. And the ellipsoid type encapsulations (HeatStixx) are better than slab type encapsulations (HeatSel), the charging and discharging time of ellipsoid type is almost 60% less than the slab type.

Comparing the two designs, submerged spiral type HX shows almost 58% more storage capacity compared with HeatStixx and 54 % more for HeatSel. But the charging and discharging time of macro-encapsulations is much faster as compared to the spiral design.

Keywords: Phase Change Material (PCM), Macro-encapsulations, Temperature-history (T-History), COMSOL Multiphysics, Latent Heat Thermal Energy Storage (LHTES), Submerged spiral type heat exchangers.

Resumo

E sabido que os materiais de mudança de fase (PCM) possuem elevada densidade de armazenamento de calor e reduzida condutividade térmica. Para validar o utilização do PCM baseado em TES (Thermal Energy Storage - Armazenamento de Energia Térmica) com o propósito de aquecimento urbano, um local de validação em escala laboratorial do LHTES (Latent Heat Thermal Energy Storage) é projetado e construído.

A seleção de um PCM comercialmente disponível e adequado para a faixa de temperatura fornecida é feita experimentalmente usando a técnica T-history. Dois tipos de permutadores de calor (HX) são projetados; HX tubo espiral em contra-fluxo submerso em PCM e HX macro-encapsulado com difusor. A baixa condutividade térmica do PCM é superada pela estrutura mecânica complexa do permutador HX. A seleção do macro-encapsulamento é feita numericamente usando o COMSOL Multiphysics 5.4.

Os ensaios T-history realizados neste estudo mostram que o Crodatherm-60 é o melhor PCM para a faixa de temperatura fornecida (46 °C - 72 °C). O permutador HX do tipo espiral submerso em PCM é projetado para estar em contra-fluxo contendo alhetas para aumentar a condutividade térmica. E os encapsulamentos do tipo elipsóide (HeatStixx) são melhores do que os encapsulamentos do tipo placa (HeatSel), o tempo de carga e descarga do tipo elipsóide é quase 60% menor que o do tipo placa.

Comparando os dois projetos, o permutador HX tipo espiral submerso mostra quase 58% maior capacidade de armazenamento em comparação ao permutador HeatStixx e 54% maior que o HeatSel. Mas o tempo de carregamento e descarregamento térmicos de macro-encapsulamentos é muito mais rápido em comparação com o design em espiral.

Palavras-chave: Material de mudança de fase (PCM), macro-encapsulamentos, histórico de temperatura (T-history), software multifísica COMSOL, armazenamento de energia térmica por calor latente (LHTES), permutador HX tipo espiral submerso.

Acknowledgments

I am also very thankful to Dr. **Rui Costa Neto**, my supervisor at IST, for all his help, support and constructive suggestions on my work. And for always being there whenever I needed help. Without his timely help and support, I wouldn't have able to complete all the paperwork required at IST.

I am also very thankful to Dr. **Carlos Augusto Santos Silva**, my co-supervisor at IST, for all his support and guidance.

I would like to take this moment to express my deepest and sincerest gratitude towards my supervisor Dr. **Justin Ning-Wei Chiu**, who supported and guided me on every step of my thesis work. I cannot thank him enough for giving me this opportunity to join his research group and accepting me as a Teaching Assistant. I really enjoyed working under his supervision and not a single day passed when I felt stressed.

I would also like to acknowledge Dr. **Saman Nimali Gunasekara** for helping me understand T-history experiments and data analysis.

I am really thankful to **Tianhao Xu**, who helped me a lot in the COMSOL simulations, experimental setup and collaborated with me in many tasks.

Furthermore, I would also like to express my gratitude to my father **Abdul Samad Gill**, for providing me with constant support and encouragement throughout my years of study. I couldn't have achieved this without my parents.

The work is done in Heat and Power division of Energy Engineering Department, KTH Royal Institute of Technology, Sweden.

I would like to thank European Union's H2020 PumpHeat project, which provided all the necessary funding for the project.

Thank you!

Yousif Muhammad

October 2019

Abbreviations

RES	Renewable Energy Source
PCM	Phase Change Material
HTF	Heat Transfer Fluid
TES	Thermal Energy Storage
LHTES	Latent Heat Thermal Energy Storage
SHS	Sensible Heat Storage
LHS	Latent Heat Storage
CHP	Combined Heat and Power
HX	Heat Exchanger
H2020	Horizon 2020
RT	Rubitherm
DTA	Differential Thermal Analysis
DSC	Differential Scanning Calorimeter
PLA	Polylactic Acid
SCDM	SpaceClaim Design Modeler

Nomenclature

$\dot{Q}$	[W]	Heat transfer rate
C_p	[J/kg.K]	Specific heat
dt	[s]	Time step
dT	[°C or K]	Temperature difference
H	[J]	Enthalpy
h	[J/kg]	Specific enthalpy
lmtd	[°C or K]	Log mean temperature difference
m	[kg]	Mass
Q	[J]	Heat
t	[s]	Time
T	[°C or K]	Temperature
U	[$W/m^2.K$]	Heat transfer coefficient
k	[W/m. K]	Thermal conductivity
A	[m^2]	Area

Table of Contents

List of Figures

List of Tables

1. Introduction

1.1. Background

The heating and cooling sector of the European Union makes up more than fifty percent of the total energy demand. Where most of the demand is met by fossil fuels which raise serious environmental concerns and security of supply issues to Europe. By supplying district heating and cooling services, and integrating RES is the only sustainable way, but demand response, the unpredictability of RES and grid balancing are some of the major challenges [1]. Thermal heat storage can increase the efficiency of the overall CHP plants and also provide flexibility in the operation. These storage units store the excess heat when the demand is low and release it when the demand is high, it can charge or discharge depending on the demand profile. The TES system integrated with the CHP enables to provide heat at faster response times and reduces the start/shutdown of the powerplants.

Phase Change Materials (PCM) are used in thermal energy storage units to store low-grade heat (30°C -250°C). Recently they have gained popularity owing to their environmentally friendly nature, high storage density, availability and their tendency to store heat even at low-temperature differences.

To address this Pump-Heat, a European-Union funded H2020 project was initiated. This project includes two Lab validations one cold and one warm, and one demonstration in IREN, Italy. The lab-scale validation rig is constructed at KTH, Sweden. At first, a suitable PCM is selected after experimental evaluation and then two types of heat exchangers are designed. A submerged spiral coil HX keeping in mind the design problems encountered in the previous units and a diffuser based filled with commercially available macro-encapsulations. Different types of capsules are simulated and then the best one is selected.

1.2. Research Objectives

The objective of this thesis is to design and prototype a lab-scale PCM based thermal energy storage system for daily heat storage, which will be used for district heating in a combined heat and power plant, that allows flexible operation.

1.3. Research Questions

The research questions for this report are as follows:

- Which PCM is suitable for the required temperature range?
- Which type of Submerged HX is suitable?
- Which type of Macro-encapsulations can be used?

1.4. Scope and Limitations

Designing, simulating and prototyping of the LHTES is done in this study. However, due to the limited time frame, the testing phase of the overall LHTES unit is not included in this study.

Ordering and procuring of the required equipments and materials is also part of this thesis work.

2. Literature Review

2.1. Thermal Energy Storage

A technology in which energy is stored either by cooling or heating in a storage material and extracted when there is a need for heating and cooling or energy production is called Thermal Energy Storage (TES). TES can regulate demand profile from short to a long period of time and improve the overall system efficiency. TES is environmentally friendly, less expensive than other storages and has a lot of applications [2]. It is basically divided into two major types; Thermal and Chemical which are further divided into different categories, Figure 1.

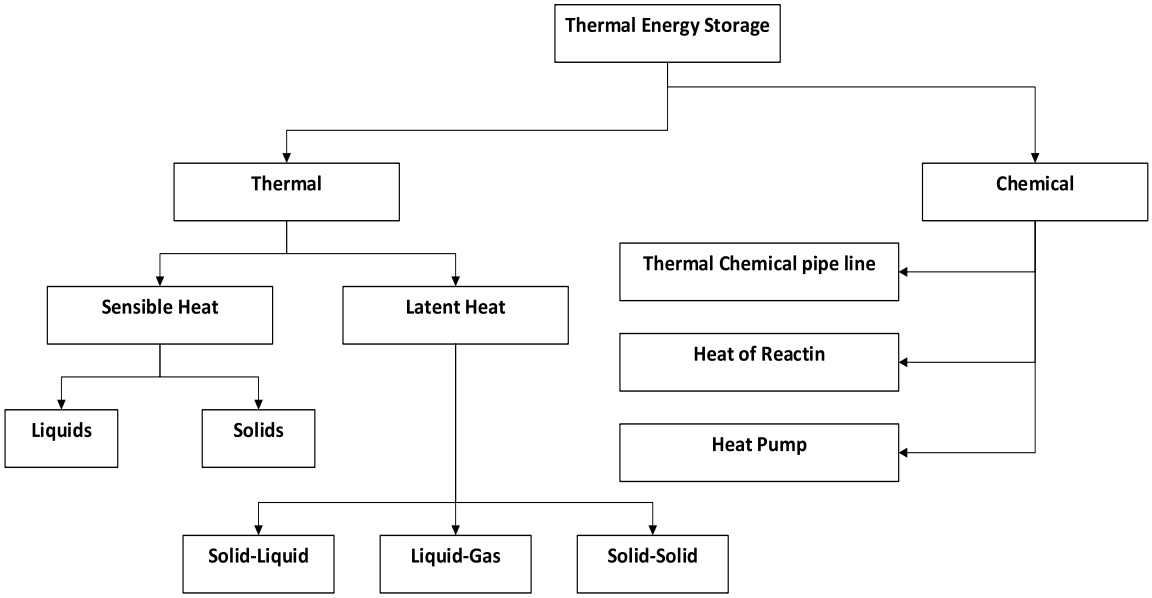

Figure 1 : Types of Thermal Energy Storage [2]

2.1.1. Sensible Heat Storage

Sensible Heat Storage (SHS) is the simplest form of heat storage, in which thermal energy is stored by either decreasing or increasing the temperature. The amount of heat stored depends upon the specific heat capacity of the material and the temperature difference between the source and storage material. Some of the common SHS materials are water, rocks, and sands. With water being the most commonly used and the cheapest option [2].

2.1.2. Latent Heat Storage

Latent Heat Storage (LHS) is a technology when the heat is being stored during the phase change period. LHS usually has high energy density and can store heat energy for a longer period of time. The amount of heat stored or released depends upon the specific heat capacity and latent heat of fusion [3].

2.2. PCM as a Storage Material

Recently phase change material has seen a huge amount of potential to be used as heat storage material even for a small temperature difference for a longer period of time [4]. It can store thermal energy for a longer period of time and it is cheaper compared to other similar technologies [2]. However, PCM has some disadvantages such as low thermal conductivity, subcooling and phase separation [5].

There are several types of commercially available PCMs with any given temperature limit, Figure 2 shows the classification of PCMs.

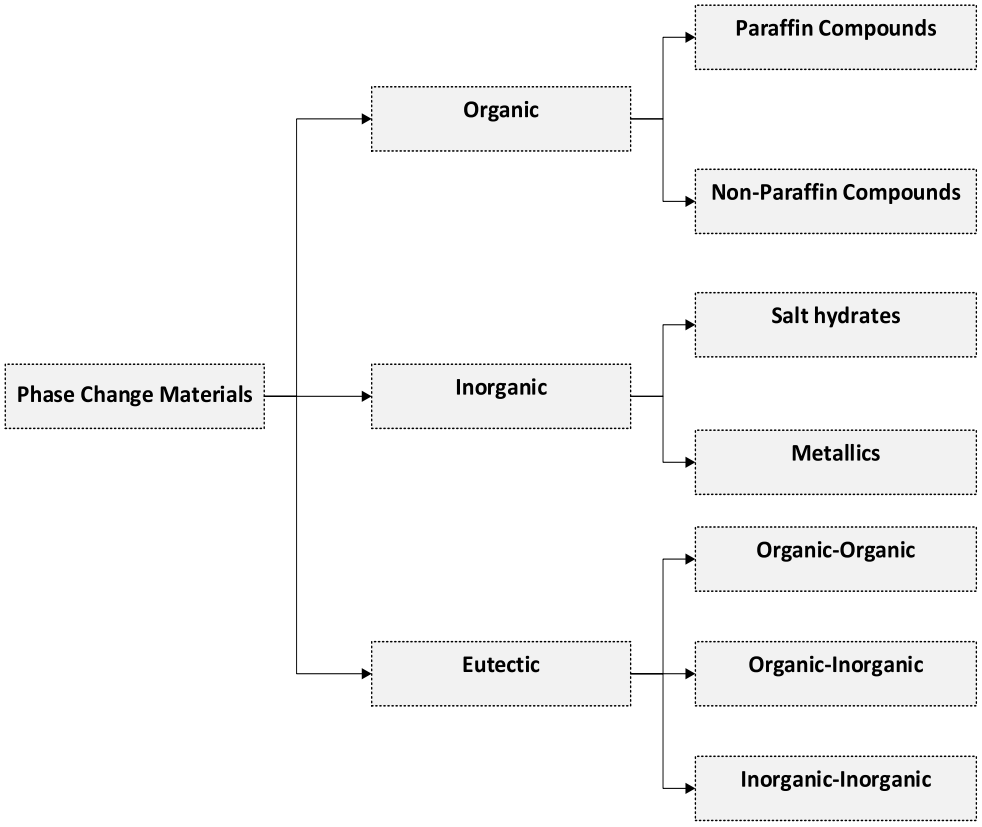

Figure 2 : Types of Phase Change Materials [5]

Paraffins and salt hydrates are the most widely used PCMs for LHTES applications. Paraffins proved to be more stable after several thermal cycles compared with salt hydrates. However, they tend to have lower thermal conductivity and enthalpy. On the other hand, salt hydrates are more prone to corrosion and show sub-cooling during the solidification process [6]. A brief comparison of these two is presented in Table 1.

Table 1 : Advantages and Disadvantages of PCM types [7]

	Salt hydrates (Inorganic)	**Paraffin (Organic)**
Advantages	• Higher density • Higher enthalpy change	• Thermally stable • Non-corrosive • Almost no sub-cooling
Disadvantages	• Less Stable • Corrosive • Sub-cooling	• Low enthalpy change • Low density • Flammable

2.2.1. Major Problems in PCM as a Storage Material

2.2.1.1. Sub-Cooling

It is a process that occurs when the PCM starts to solidify before reaching its melting temperature which results in lower thermal storage efficiency. And if it becomes severe it may not release heat at all, Figure 3 (b).

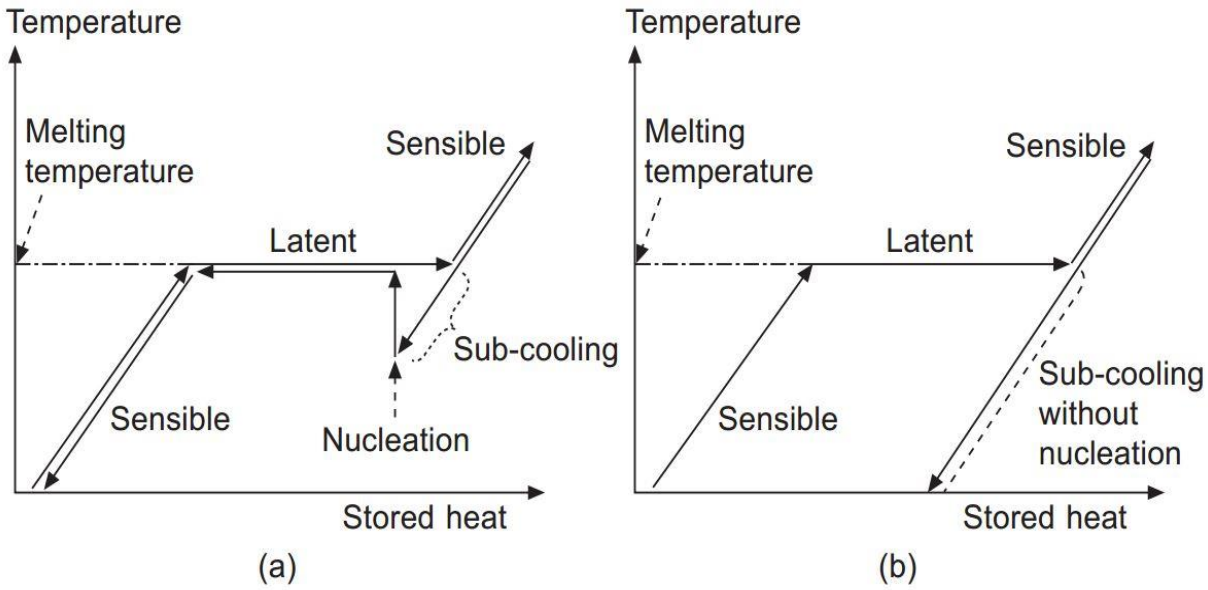

Figure 3 : Sub-Cooling behavior of PCM; (a) Sub-cooling after nucleation, (b) Sub-cooling without nucleation [3]

2.2.1.2. Phase Separation

Salt hydrates usually melt to produce a mixture of properly hydrated salt and anhydrous form of salt, this is known as phase separation or incongruent melting. This is the main reason behind the less thermal stability of the salt hydrates [8].

2.3. Types of Heat Exchangers

In order to integrate PCM as a storage material into the system, a container that will also be used as the heat exchanger is introduced. There is a large variety of heat exchanger containers that can be used for this purpose, but generally, for LHTES submerged HX and diffuser (macro-encapsulation) tanks are preferred depending on the system requirement.

For submerged HXs most commonly heat transfer area and the inlet temperature determines how fast is the charging and discharging process [9], [10]. After experimenting with five different types of HX, the one with the largest heat transfer area has the highest power. But when the comparison is made based on the power per unit area, double pipe with graphite matrix attached to it has the highest value [10]. Some of the recent models are discussed in this chapter.

2.3.1. Spiral Type Heat Exchanger

A spiral coil heat exchanger was designed and tested in a study [11], the model consisted of eight coils which are counter-flow with any adjacent coils and has four vertical tubes for hot and cold Heat Transfer Fluid (HTF), two at the center and two at the boundary of the tank, as shown in Figure 4. It was encountered in the experimental process that 25 % of PCM was a dead mass, meaning that only the PCM close to the coils is affected by the temperature difference [11].

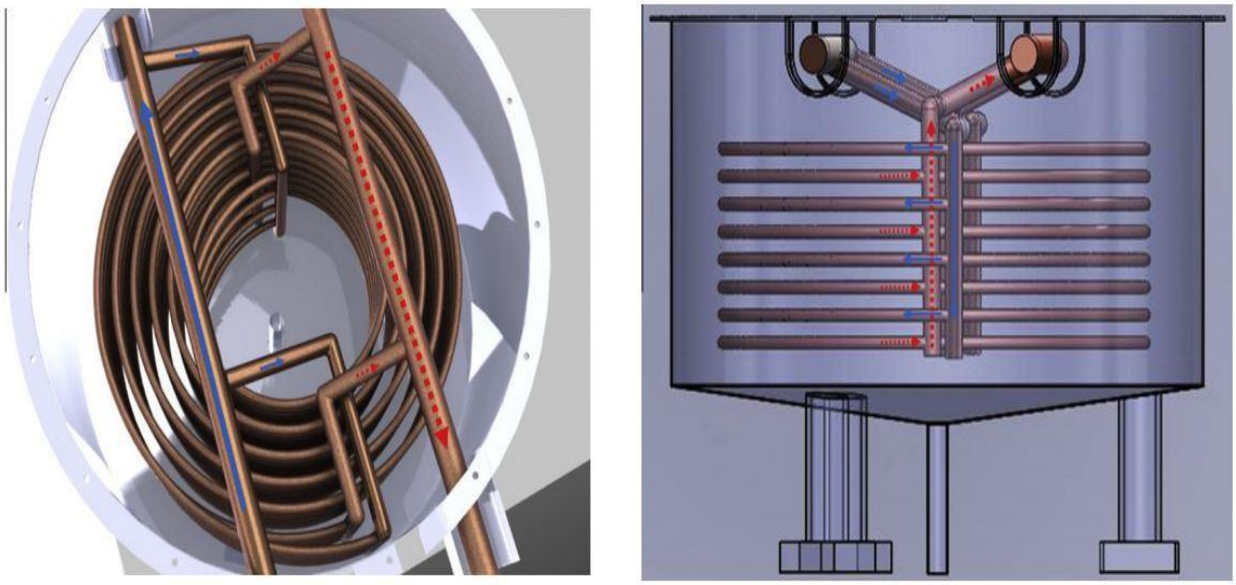

(a) Top View (b) Side View

Figure 4 : Spiral type HX [11]

2.3.2. Straight Pipe with Spiral Fins Heat Exchanger:

Another model of the heat exchanger with straight copper tubes consisting of spiral wire fins was simulated and tested [12], Figure 5. In this study, the HX gives satisfactory results, but the overall heat capacity is decreased owing to the large spiral fin area which reduces the amount of PCM in the HX. Furthermore, it was noticed during the solidification process a layer of solid PCM is attached to the fin area, the thickness of which increases with the solidification process. This layer provides the thermal resistance which will slow down the solidification process. After taking double the time of charging, only 75% of PCM solidifies [12].

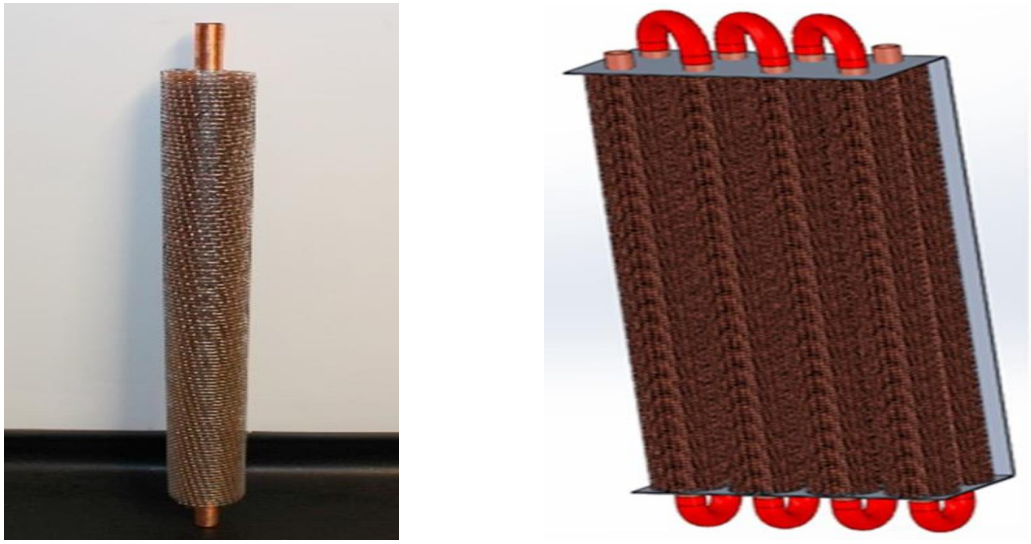

(a) Copper pipe with spiral fins (b) CAD model of HX

Figure 5 : Spiral finned shell and tube HX [12]

2.3.3. U-Tube Shell and Tube Heat Exchanger

Experimental performance evaluation was performed on vertical U-tube shell and tube heat exchanger [9], in this study horizontal and vertical orientation of the model was tested, as shown in Figure 6. For the charging phase, the horizontal orientation was found to be more effective since it promotes natural convection, while for the discharging it's not that different. It also states that the temperature difference is one of the main driving factors. In the absence of fins, the charging and discharging time will be much higher and PCM in the area close to the boundary of the cylinder will be a dead mass.

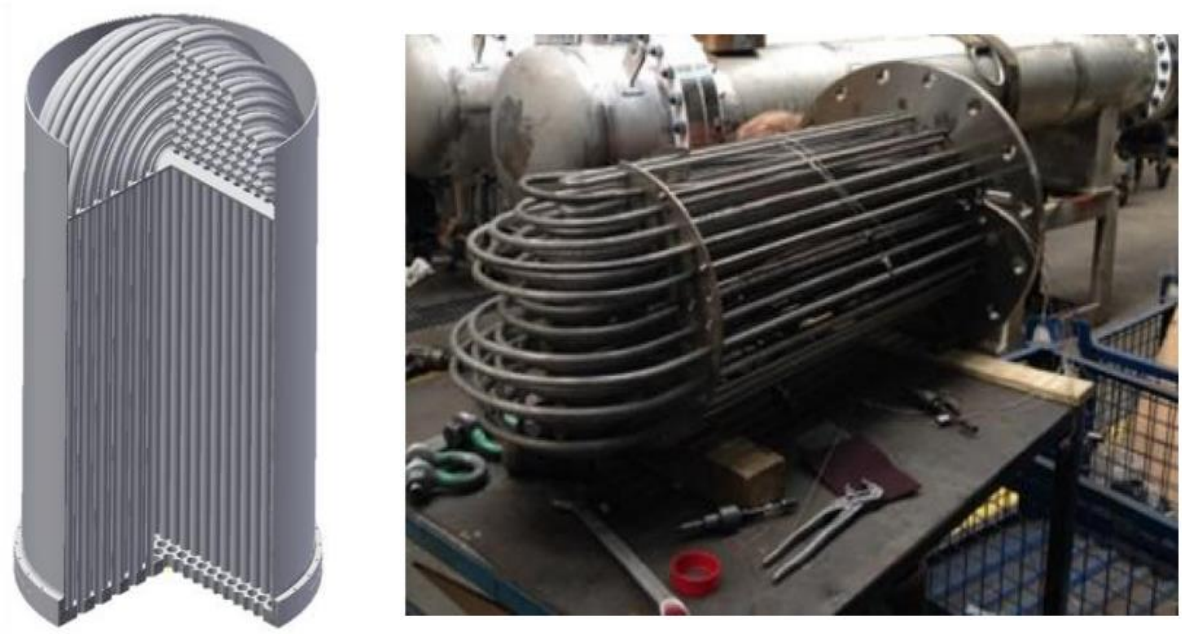

(a) CAD view (b) Real Model

Figure 6 : U-Tube shell and tube HX [9], [13]

2.3.4. Macro-Encapsulated Heat Exchanger

The model of a macro-encapsulated heat exchanger is very simple, capsules (plastic, metal) filled with PCM are added layered into a container having two diffusers, one at the top and one at the bottom. The performance of a macro-encapsulated HX depends on a number of factors; capsule type, shape and size, void fraction, type of PCM, properties of HTF (flow rate, heat transfer coefficient) and tank design [14]. A generic macro-encapsulated tank is shown in Figure 7.

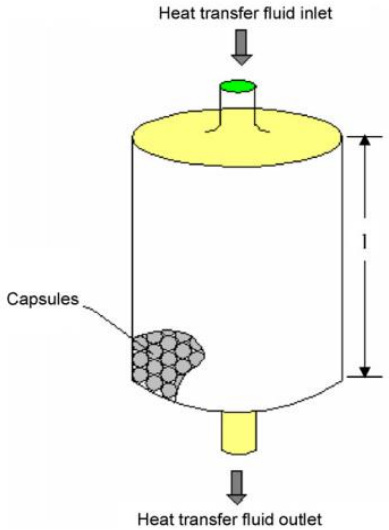

Figure 7 : Storage tank with Macro-Encapsulations [14]

2.4. Heat Storage Capacity of PCM Storage Tank

The amount of heat stored in a storage tank is a vital parameter when designing an LHTES. The total heat stored is a sum of sensible heat and latent heat. Mostly the heat storage capacity depends upon the mass of PCM and the thermal properties of PCM, such as specific and enthalpy of fusion. The total heat stored in the tank throughout its temperature range is given in the Eq (1), [15].

$$Q = m\,[C_{p,s}(T_m - T_i) + \Delta h_{s-l} + C_{p,l}(T_f - T_m) \quad (1)$$

Where, $C_{p,s}$ and $C_{p,l}$ are the specific heats during their liquid and solid phase, T_i, T_m, and T_f are the initial, melting and final temperatures of a PCM respectively, and Δh_{s-l} is the enthalpy change during the phase change (solid-liquid or liquid-solid) or simply called the latent heat of fusion. Mass multiplied by the latent heat of fusion gives the latent heat stored and the rest gives sensible heat stored in the storage tank, [15].

3. Methodology

3.1. Storage Material Selection

Selection of a suitable storage material is one of the most important tasks of this thesis, different types of PCM are evaluated based on different criteria. Some of which are given below [16], [17]:

- High Storage Density
- Good heat conductivity
- Phase Change temperature should be within the operating temperature
- Zero or minimum subcooling

Since this thesis is under the framework of PumpHeat project, the charging temperature of 72°C will be provided by the heating source at IREN [18]. It was noted in the inspection of the heat pump that the heat pump can run at a low evaporator temperature of 46°C. If we take a pinch temperature of 3°C, the operating temperature of TES will be between 49°C and 69°C, as depicted in Figure 8. But to get three times faster discharge rate while operating within these temperature ranges the ideal phase change temperature should at 62.3°C, by using lever rule for the given temperature range. Since the commercially available PCMs do not have a sharp phase change temperature, PCMs having 59±3 °C phase changer temperature will be shortlisted for our application.

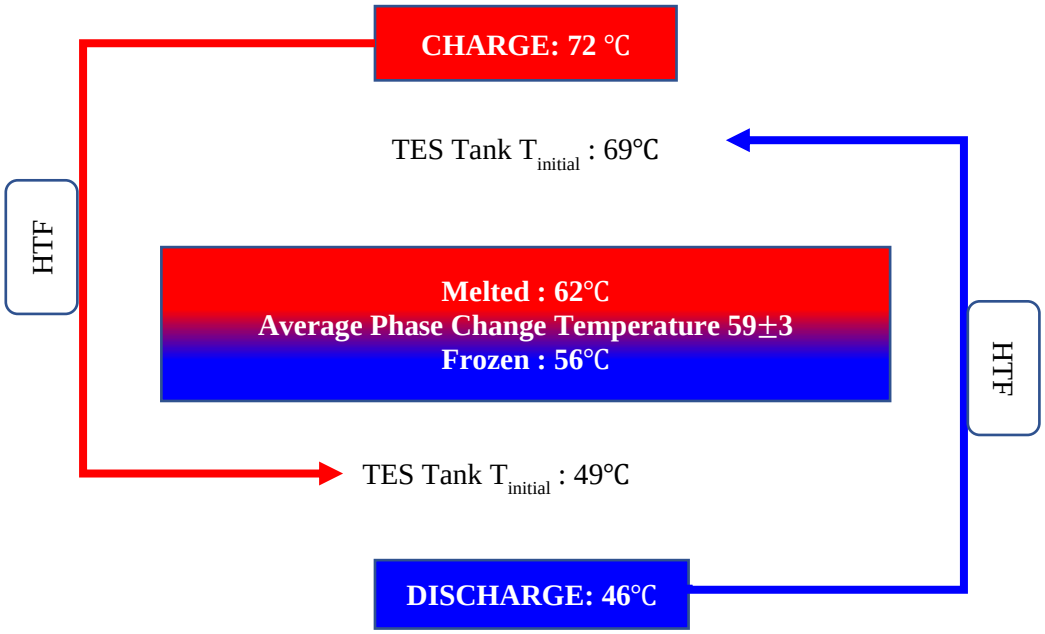

Figure 8 : Operating Temperature Range of PUMPHEAT; Heat Transfer Fluid (HTF) [13]

3.1.1. Shortlisted PCMs

Keeping in mind the previously described criteria and the temperature range, five commercially available PCMs were shortlisted. Among them three were organic (Paraffin) and two inorganics (Salt hydrates), RT-60, RT-64HC from Rubitherm; CrodaTherm-60 from CRODA; SU-58 from SunAmp; ATS-58 from Axiotherm. Table 2 shows some of the important characteristics of the shortlisted PCMs, these values were taken from the datasheet provided by the supplier[1].

Table 2 : Thermal Properties of Shortlisted PCMs

Product Name	Phase Change Temperature (°C)	Heat Storage Capacity (kJ/kg)	Thermal Conductivity (W/m.K)	Specific Heat Capacity (kJ/kg.K)	Density (kg/m3)
RT-62HC	62 ± 1	230	0.2	2	845
RT-64HC	64 ± 2	250	0.2	2	830
CrodaTherm-60	60 ± 3	217	0.29	2.3	873
SU-58	58 ± N/A	226	N/A	3	1200
ATS-58	58 ± 2	240	0.6	3	1280

3.1.2. Temperature -History Testing

The properties stated in Table 2 are extracted from the data sheets provided by the suppliers. These thermal properties are very vital for designing the thermal energy storage systems, to have a better idea of available thermal capacity and charging/discharging rates. Most of the values provided by the suppliers are obtained by using traditional evaluation

[1] Data Sheets can be found in Appendix-1

methods such as differential scanning calorimeter (DSC) and differential thermal analysis (DTA). T-history is a recently developed method for evaluating enthalpy and heat capacity which can be used for non-homogeneous samples showing subcooling behavior. Because of this method was used in this study to five shortlisted samples. A short description of this method is given in this study.

3.1.2.1. Fundamental on T-History method

T-history basically consists of a comparison between a reference sample whose material properties are known and a test sample. The T-history used in this study is based on [19], [20]. The reference Stainless-steel tube whose thermal properties such as heat capacity and heat conductivity are known is used to measure the heat accumulated over the sample period, as in Eq. (2). The total heat gained can be curve fitted using logarithmic mean temperature difference, Eq. (4) and Eq. (5) [21]. Overall heat transfer coefficients k1 Eq. (6) are the same for the reference and test samples, since the geometry and dimensions of a Stainless-steel reference tube and PCMs filled in SS test tubes are identical. By back calculations, the total heat gained (Q_{tot}) can be evaluated, Eq. (8), which the heat is gained by PCM and SS test tube, as in Eqs. (9) and (10). Heat gained by the SS test tube is calculated by using the Eq. (7) which is then subtracted from the Q_{tot} to obtain the heat gained by PCM samples. Using this we can back-calculate the enthalpy of the PCM, using Eq. (12). The specific heat Cp of these PCM samples were obtained using the enthalpy obtained in the previous, by following the Eq. (13). Total thermal energy storage capacity of the samples is calculated using Eq. (14) for a given temperature range (T_1-T_2).

$$\dot{Q}_{SS\_S} = m_{SS\_S} \cdot \frac{dH_{SS\_S}}{dt} = m_{SS\_S} \cdot C_{P,SS\_S} \cdot \frac{dT_{SS\_S}}{dt} \tag{2}$$

$$\dot{Q}_{SS\_S} = k_1 \cdot lmtd_{SS\_S} \tag{3}$$

$$lmtd_{SS} = \frac{[\left({T_{SS\_S}}^{n-1} - {T_{Box,amb}}^{n-1}\right) - \left({T_{SS\_S}}^{n} - {T_{Box,amb}}^{n}\right)]}{\ln[\frac{\left({T_{SS\_S}}^{n-1} - {T_{Box,amb}}^{n-1}\right)}{\left({T_{SS\_S}}^{n} - {T_{Box,amb}}^{n}\right)}]} \tag{4}$$

$$lmtd_{PCM} = \frac{[\left({T_{PCM}}^{n-1} - {T_{Box,amb}}^{n-1}\right) - \left({T_{PCM}}^{n} - {T_{Box,amb}}^{n}\right)]}{\ln[\frac{\left({T_{PCM}}^{n-1} - {T_{Box,amb}}^{n-1}\right)}{\left({T_{PCM}}^{n} - {T_{Box,amb}}^{n}\right)}]} \tag{5}$$

$$T_{SS\_TT} := T_{PCM} \Rightarrow lmtd_{Tot} = lmtd_{SS\_TT} = lmtd_{PCM} \tag{6}$$

$$U\,.A = \frac{\dot{Q}_{SS\_S}}{lmtd_{SS\_S}} = \frac{\dot{Q}_{Tot}}{lmtd_{Tot}} = \frac{\dot{Q}_{PCM} + \dot{Q}_{SS\_TT}}{lmtd_{PCM}} \tag{7}$$

$$\dot{Q}_{Tot} = \dot{Q}_{PCM} + \dot{Q}_{SS\_TT} = k_1 \cdot lmtd_{PCM} \quad (8)$$

$$\dot{Q}_{SS\_TT} = \dot{m}_{SS\_TT} \cdot C_{P,SS\_TT} \cdot dT_{SS\_TT} \quad (9)$$

$$\dot{Q}_{PCM} = k_1 \cdot lmtd_{PCM} - \dot{Q}_{SS_{TT}} \quad (10)$$

$$\dot{Q}_{PCM} = k_1 \cdot lmtd_{PCM} - \dot{m}_{SS\_TT} \cdot C_{P,SS\_TT} \cdot dT_{SS\_TT} \quad (11)$$

$$h_{PCM} = \frac{\dot{Q}_{PCM} \cdot dt}{m_{PCM}} \quad (12)$$

$$\frac{dh(T)}{dt} = \frac{C_P(T) \cdot dt}{dt} \quad (13)$$

$$Q_{PCM} = \int_{T1}^{T2} m \cdot dh_{PCM}(T) = \int_{T1}^{T2} m \cdot C_{P,PCM}(T) \cdot dT \quad (14)$$

3.1.2.2. Experimental Setup:

The selected PCMs were poured in the stainless-steel test-tubes after melting them in an electric furnace and then labeled. The reference tube is a solid Stainless-Steel tube with the same dimensions and shape as the test sample was selected. After pouring the materials in the test tube the two thermocouples were placed inside the test tubes almost to the center of the tube. It is made sure that the thermocouples reach almost to the center of the test tube for the PCM samples and for the reference test tube these thermocouples are attached to the body of the test tube. Then they are insulated using a 19 mm thick High-Temperature Armaflex cover which is specially cut to accommodate these types of test tubes. These insulated tubes were laid down on the test container and then the container is closed using screws. All these tasks are done to keep the Biot number less than 0.1, which is a requirement for using T-history experiments. This container was then placed in an ACS Hygross 1200 climate chamber, where it was thermally cycled between four heating and cooling cycles respectively between the temperature range of 45°C - 80°C with the ramp of 0.1 K/min, Figure 9. The schematic of the experimental setup is shown in Figure 10 (a) and the SS tube along with the armaflex insulation is shown in Figure 10 (b) and (c).

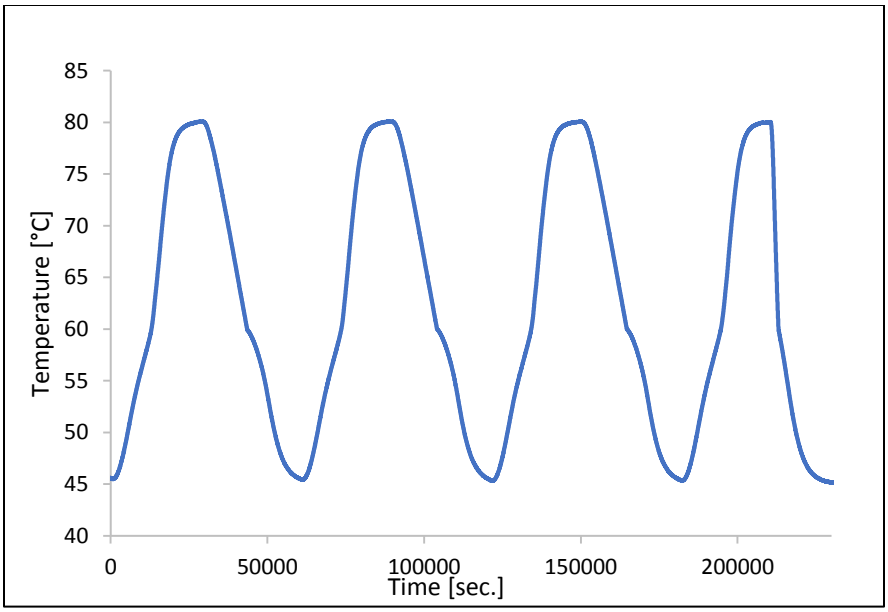

Figure 9 : Temperature input to the Climate Chamber

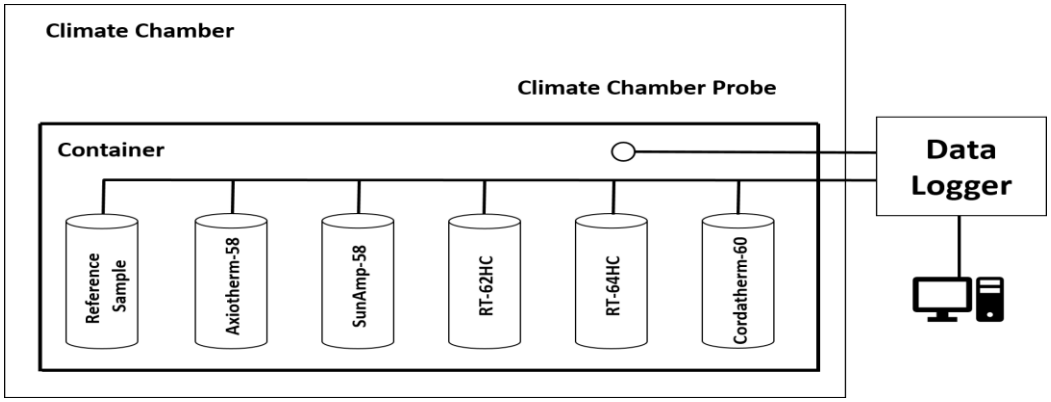

(a) Schematic of T-History test

(b) SS test

(b) SS test tubes insulted by Armaflex

Figure 10 : Experimental Setup of T-History

A measured amount of PCM is carefully inserted in the SS test tubes using a sensitive weighing scale. The weight of the test samples and test tubes is given in Table 3. It can be

noticed from the given Table 3 that the salt hydrate based PCMs are usually heavier than the paraffin ones.

Table 3 : Weights of PCMs inside test tubes

Test Material	Test Tube + PCM (g)	PCM (g)
Axiotherm-58	74.17	13.87
SunAmp-58	74.10	13.91
RT-62HC	69.60	9.12
RT-64HC	69.57	9.12
Crodatherm-60	69.25	8.86

3.2. Heat Storage Tank Design

Designing a heat storage tank which will also act as a heat exchanger was also an integral part of this study. Given the limitation of the laboratory space few constraints related to the size of the tank were there. Designing and modeling of the tank are done using Solid Edge ST 10, keeping in mind all the limitation and requirements, Figure 11. The model was basically a scalled down version of the storage tank which will be used a the demonstration site in Italy, so the height to diameter ratio is kept similar to that of demonstration site which was 2. And the height of the storage was kept 2660 mm because the ceiling of the laboratory was 3000 mm. All the measurements are in mm.

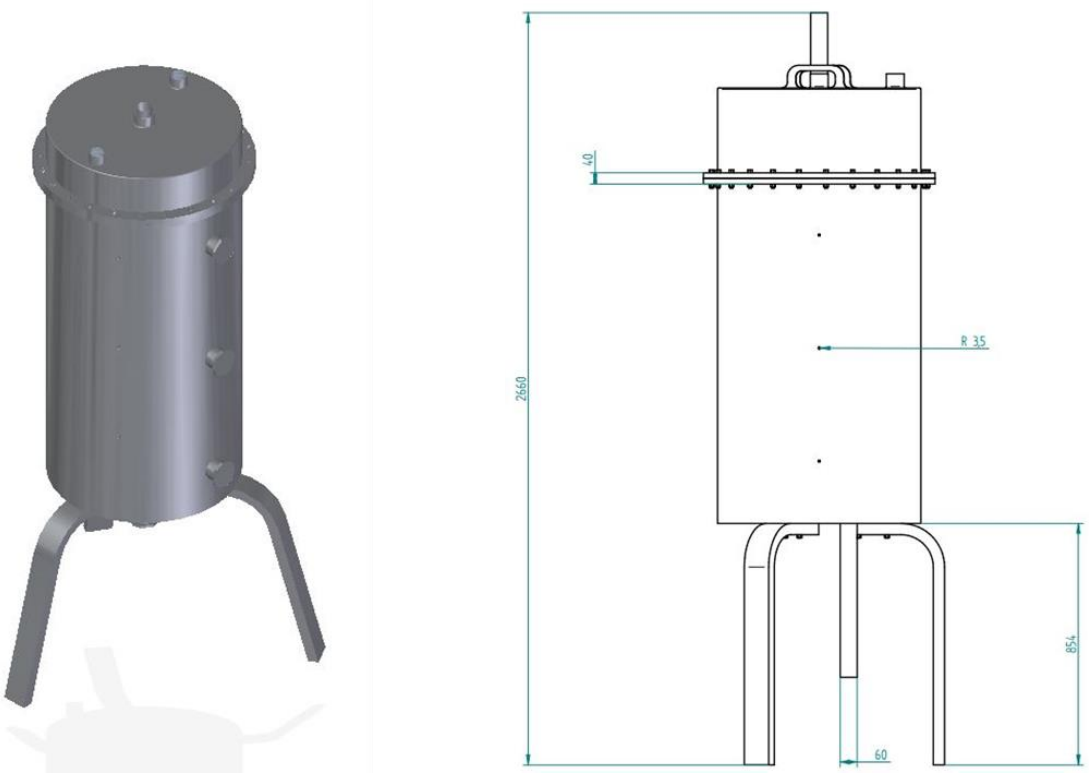

(a) (b)

Figure 11: Heat Storage Tank; (a) CAD model, (b) Detailed tank with measurements

This study mostly focuses on the internal part of the tank which will act as a heat exchanging medium. Two different configurations were designed which be placed in the above-mentioned tank: (1) Shell-and-tube spiral type with Heat Transfer Fluid (HTF) in the tube and PCM in the shell and (2) Diffuser based with many encapsulations stacked in the tank and water flowing through it. The rough idea of the two configurations are shown in Figure 12 and will be discussed in detail later in this chapter.

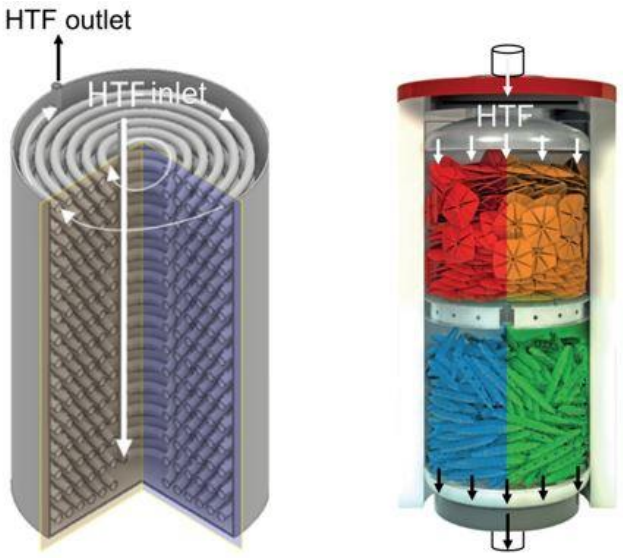

Figure 12 : Possible configurations of LHTES tanks; (a) Spiral coil configuration [13], *(b) Tank filled with Axiotherm Encapsulations*[2]

3.2.1. Submerged Spiral Type HX Storage

The first design consisted of two pipes one at the center and the other at the inner periphery of the external tank. The model is oriented vertically, and the spiral copper tubes are placed concentrically to the tank and the center pipe. The Heat Transfer Fluid (HTF) will enter from the center pipe and distribute equally among all the spiral tube levels, where after circulating will ultimately exit close to the inner periphery of the outer tank in the side pipe. The number of turns and the pitch between the turns and the different levels correspond to the heat transfer surface and the maximum heat capacity. A sensitivity analysis was done on the pitch between the coils and the rows, to keep the balance of heat transfer surface and the heat capacity a pitch of 50 mm was decided for the turns and between the levels. Both the spiral coils and the pipes are made of copper. Initially, the diameter of the pipes is kept to 100 mm and the thickness of 2 mm. The dimensions of the copper tubes and the inlet and outlet pipe were selected by keeping in mind the products which were easily available on the market.

By putting the pitch of 50 mm between different turns of the coil and the end diameter, an automatic tube having five turns was generated from the Solid Edge. The same procedure was applied to generate different levels of the spiral by inputting the length of the center pipe and the pitch, which resulted in fifteen levels, as illustrated in Figure 13.

[2] Data sheet presented in Appendix-3

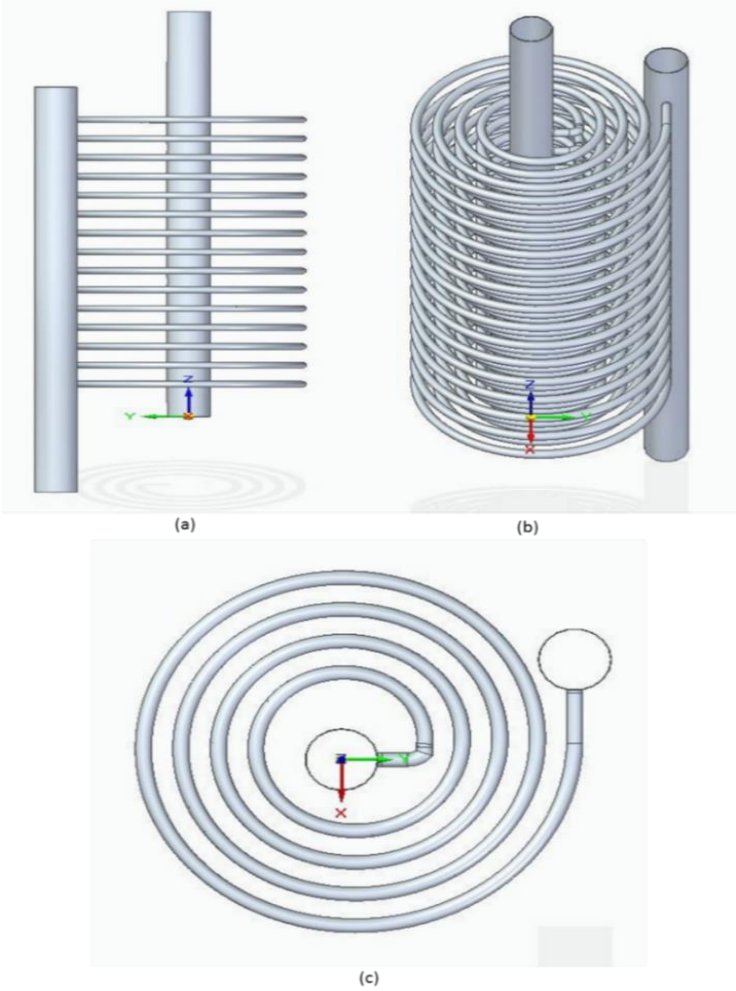

Figure 13 : Initial Submerged HX design; (a) Side View, (b) Isometric view and (c) Top view

But the heat transfer simulations done on the COMSOL for this model which is not part of this study, show that the heat transfer rate was very low. The PCM didn't even melt after two hours of charging. Moreover, since the pitch between the spiral coil was large which resulted in very slow phase change and especially the area close to the center pipe and the boundary of the tank didn't undergo any phase change.

3.2.1.1. Final Design

After looking at the constraints and talking with the suppliers, changing the orientation of the inner structure and decreasing the pitch between the turns to 40 mm and among different levels to 35 mm is the easiest and the most efficient way. The main idea behind this new design was to utilize all the space within the tank effectively and to have a counter-flow which will increase the heat transfer area. Now there were three pipes instead of two, one at the center and another two at the opposite sides of the inner periphery of the tank. And the coils were not anti-clockwise in direction anymore, in fact, it was a mixture of clockwise and anti-clockwise, Figure 14.

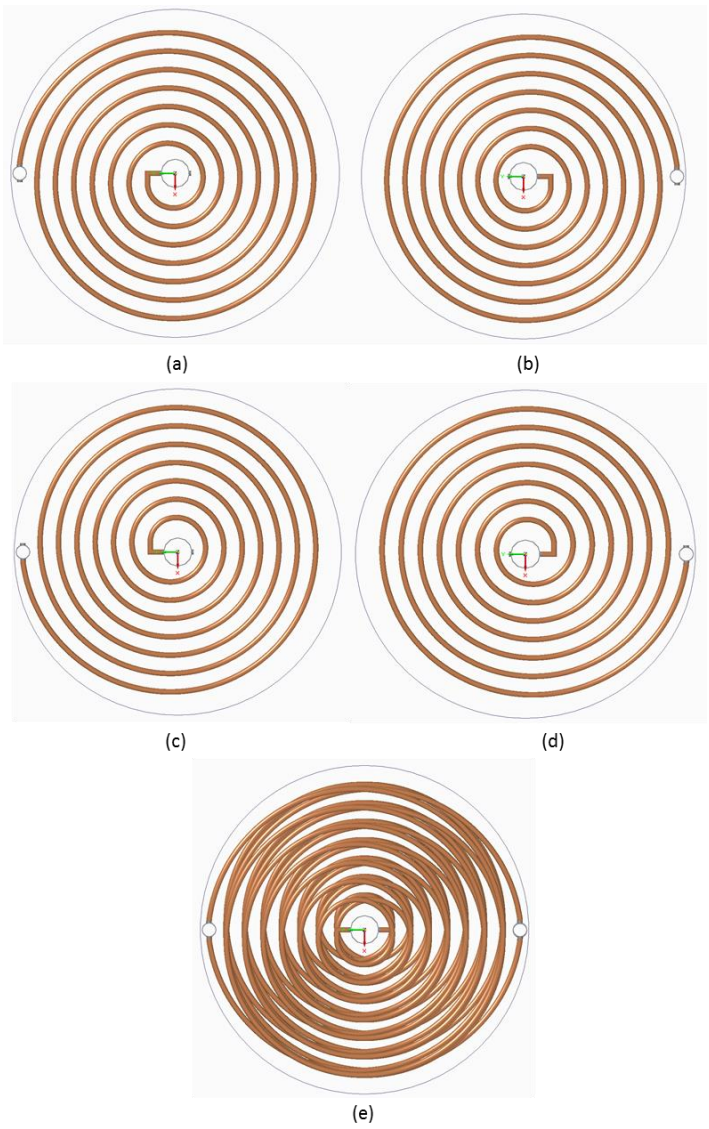

Figure 14 : Top view of final inner version; (a) First row, (b) Second row, (c) Third row, (d) Fourth row and (e) Top view

The same procedure was applied to get the number of turns and the number of spiral levels[3], which resulted in eight turns and thirty-six levels, Figure 14. Holes were generated on either side of the center pipe with the first hole on the left side and the second one on the right side which are 35 mm apart vertically. The first row starts from the left side of the center pipe and rotates in an anti-clockwise direction Figure 14(a), while the second row starts from the right side and rotates in a clockwise direction. In the third and fourth row, the pattern is reversed, with third-row starting from the left side and rotating in a clockwise direction and the fourth row starting from the right side rotating in an anti-clockwise direction. After this, the pattern of four levels is repeated for nine times making thirty-six levels, as visible in Figure 15 where the side view of the final structure is presented. This

[3] Detailed schematic of coil is present in the Appendix-4

heat exchange design was merely designed to utilize all the possible space without decreasing the amount of PCM inside the tank. Moreover, counter-flow tends to have a good effect on heat transfer coefficient [11].

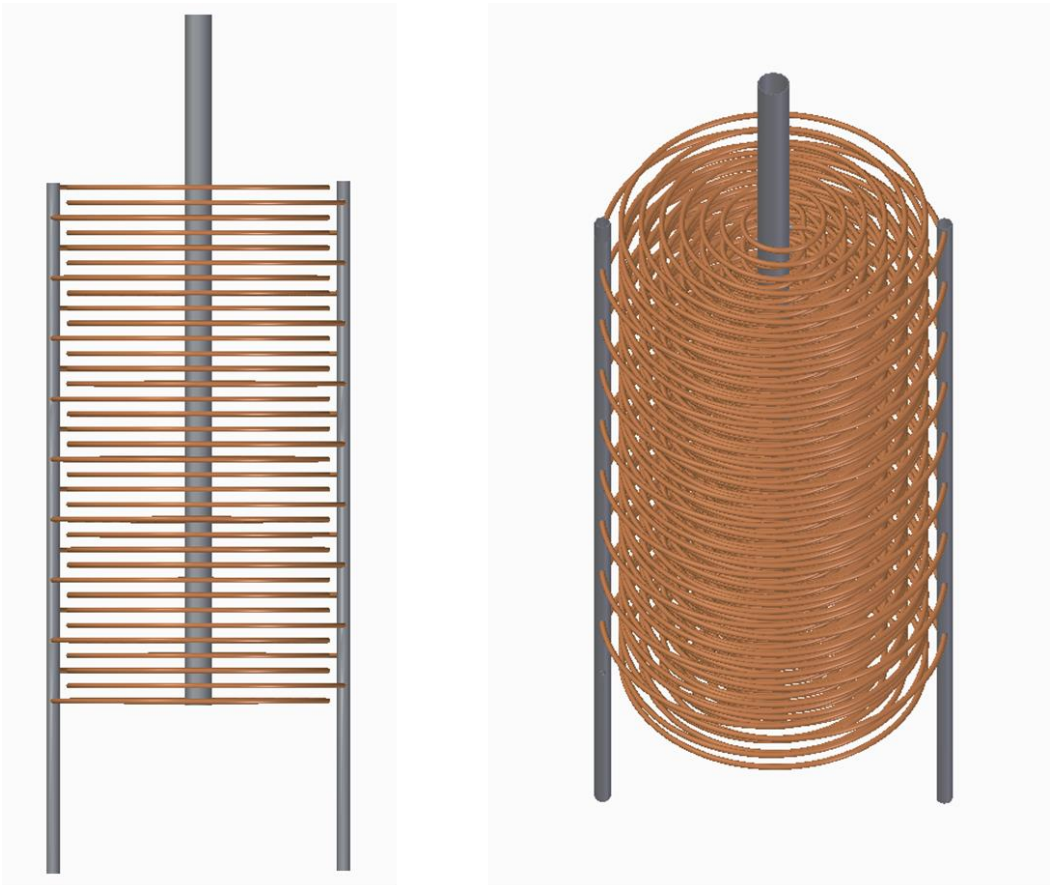

Figure 15 : Final CAD model; (a) Side View, (b) Isometric view

3.2.2. Encapsulated Tank Design

The designing and modeling of macro-encapsulated PCM storage tank was also part of this study in which various marco-encapsulation options were analyzed and simulated. The size and shape of the encapsulation play a vital role in the performance of LHTES. Larger encapsulations will have higher thermal energy storage capacity but the charging and discharging rate will be much slower, while in smaller encapsulations the rate of charging and discharging faster but they have much lower thermal energy storage capacity [22]. According to the study done previously on this project, it was suggested that capsules of 60 mm height and 30 mm diameter will be suitable for the given working temperature range [18]. A sample of one capsule which will also be used as an input to the 3-D printer is shown in Figure 16.

Figure 16 : Capsule CAD for 3-D printer

To find a suitable supplier who could provide these custom-made capsules was an impossible task, the only option was to manufacture them in the lab using 3-D printers. One 3-D printer was also bought for this purpose, but then after doing some estimations, it was clear that 3-D printer will take approximately five to six months to produce the required number of capsules if run continuously without any interruption. Moreover, Polylactic Acid (PLA) which is used as a printing material has a melting temperature between 150 to 160 °C, but there may be deflection in the shape due to heat at a much lower temperature of around 60°C [23].

Now the only option left was to have something which was commercially available in the market. Two types of commercially available marco-encapsulation provided by Axiotherm GmbH were analyzed using COMSOL Multiphysics 5.4 to check their performance under the given conditions because there is no performance evaluation data available.

3.2.2.1. Simulation Model Setup

This section will explain how the encapsulations are modeled and the procedure through which different material properties were set up in the simulation. SpaceClaim Direct Modeler (SCDM 2019) is used to model the encapsulations and COMSOL Multiphysics 5.4 is used to study the heat transfer inside these encapsulations. Some groves and cuts were ignored during the modeling for the sake of simplicity.

Two-dimensional study of these encapsulations is not enough, to fully study the behavior of these encapsulations a three-dimensional study is performed using heat transfer physics in a time-dependent study. Heat transfer study in COMSOL is not based on enthalpy rather it is based on heat transfer coefficient, specific heat capacity, thermal conductivity and density of the material. The physical properties of both the cover and PCM are temperature dependent. The physical properties of the cover which is poly-propylene can be obtained from the built-in material library in the COMSOL. Initially both the cover and PCM are kept at 49°C (322 K) and a heat flux having heat transfer co-efficient of 123 $W/m^2.K$ at 72°C (345 K) is applied at the boundary of the capsule to check the performance equation, which is then run for a period of two hours with physically controlled time interval. The

values for the PCM were added manually using the data sheets[4] and the T-history measurements. The specific heat capacity graph is shown in Figure17 (a) was adapted from the T-history results performed earlier in this study. Crodatherm-60 has a thermal conductivity of 0.29 W/m.K when solid and 0.17 W/m.K when liquid[5]. Hence, 0.29 W/m.K is set constant for the solid phase until 55°C, and 0.17 W/m.K from 65°C when it is completely liquid, the region between these points where the phase change takes place is linearly interpolated. This provides an approximation of thermal conductivity at any given temperature between them, Figure 17 (b). A similar procedure was applied to obtain a density graph where it was linearly interpolated between 922 kg/m^3 at 55°C and 824 kg/m^3 at 65°C, Figure 17 (c).

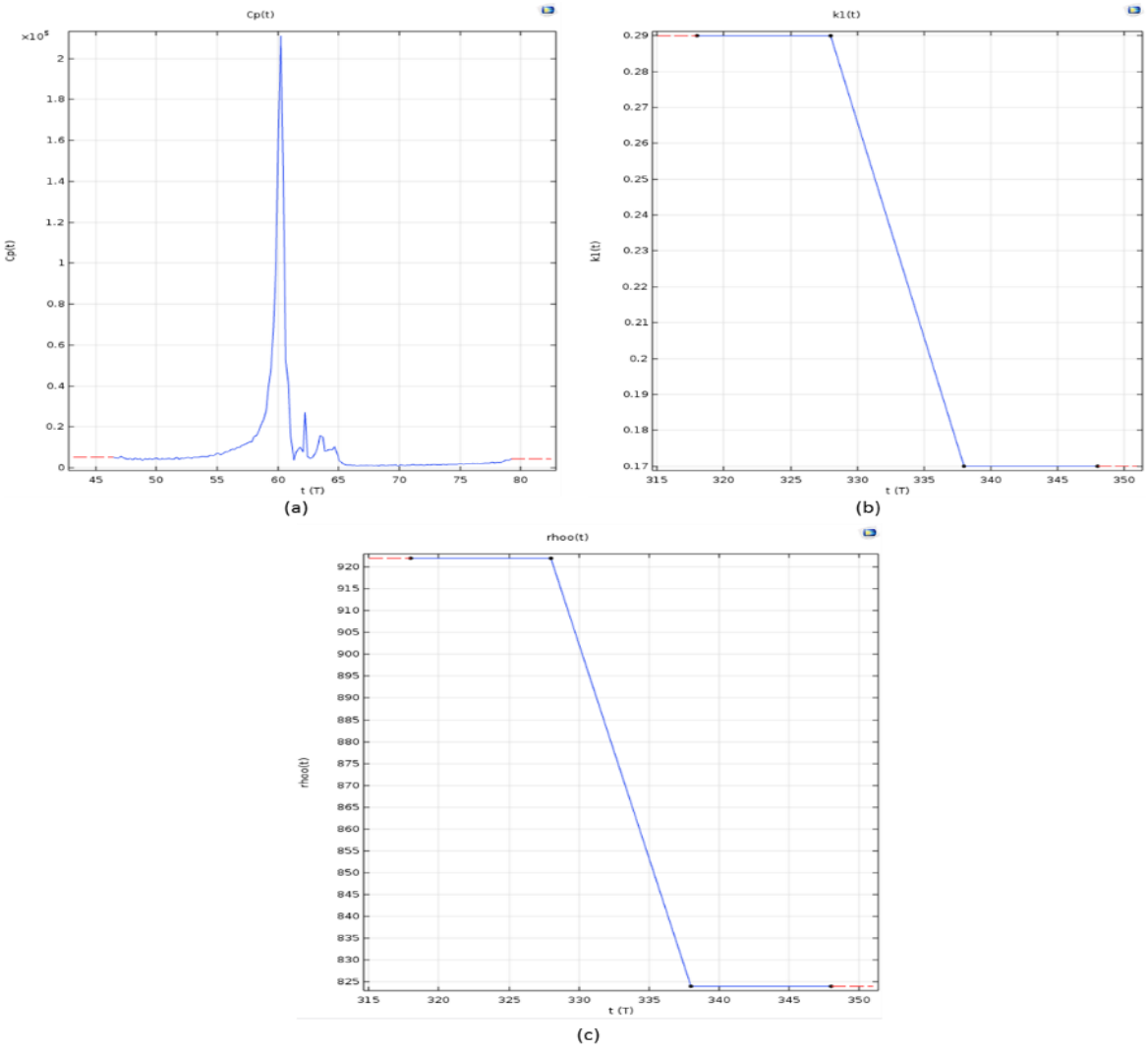

Figure 17 : Input thermal properties w.r.t temperature in COMSOL; (a) Specific heat capacity, (b) Thermal conductivity, and (c) Density

[4] Data sheets in Appendix-1
[5] Datesheets in the Appendix-1

3.2.2.2. HeatStixx (Ellipsoidal Shaped)

The First encapsulation was shaped like an ellipsoid with several groves engraved in the model known as HeatStixx. The capsule is made up of 2 mm thick Polypropylene (PP) plastic. The capsule has a diameter of 0.04 m and a length of 0.3 m, whereas the volume of 245 mL was measured manually at the lab. They have a surface area if 0.062 m^2 and it can accommodate almost 0.21 kg of PCM (Crodatherm-60). The model is basically a simplified version of the capsule, where the small cuts and groves are neglected for the sake of simplicity except the two deeper ones on either side. The model used for computation and the meshing is shown in Figure 18.

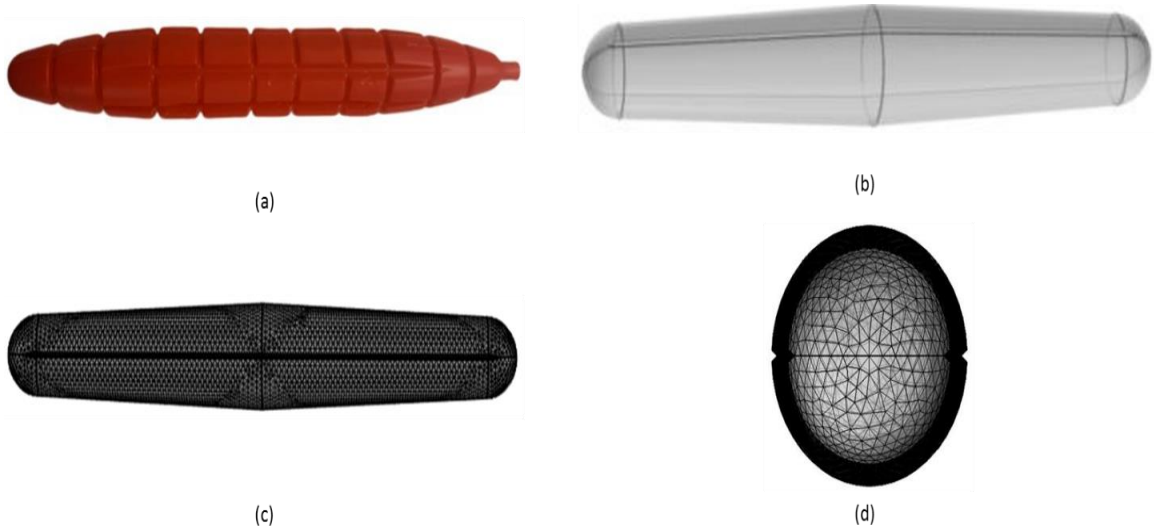

Figure 18 : Illustration of HeatStixx; (a) HeatStixx capsule, (b) Approximated CAD model, (c) Side view in computational model, and (d) Top view in computational model

3.2.2.3. HeatSel (Slap with Curved Edges)

The second encapsulation is somewhat similar to a slab with curved edges having several cuts diagonally and bisectionally, known as HeatSel. The capsule is made up of 2 mm thick Polypropylene (PP) plastic. It has a height and length of almost 0.2 m and an internal volume of 350 mL. The surface area of this capsule is 0.085 m^2, almost 28% more than HeatStixx. It can accommodate almost 0.31 kg of PCM (Crodatherm-60). The thickness of this slap is different along the length which can be seen from the cross-sectional view in Figure 19 (d). An approximated 3-D model and the meshing of a cross-section is shown in Figure 19.

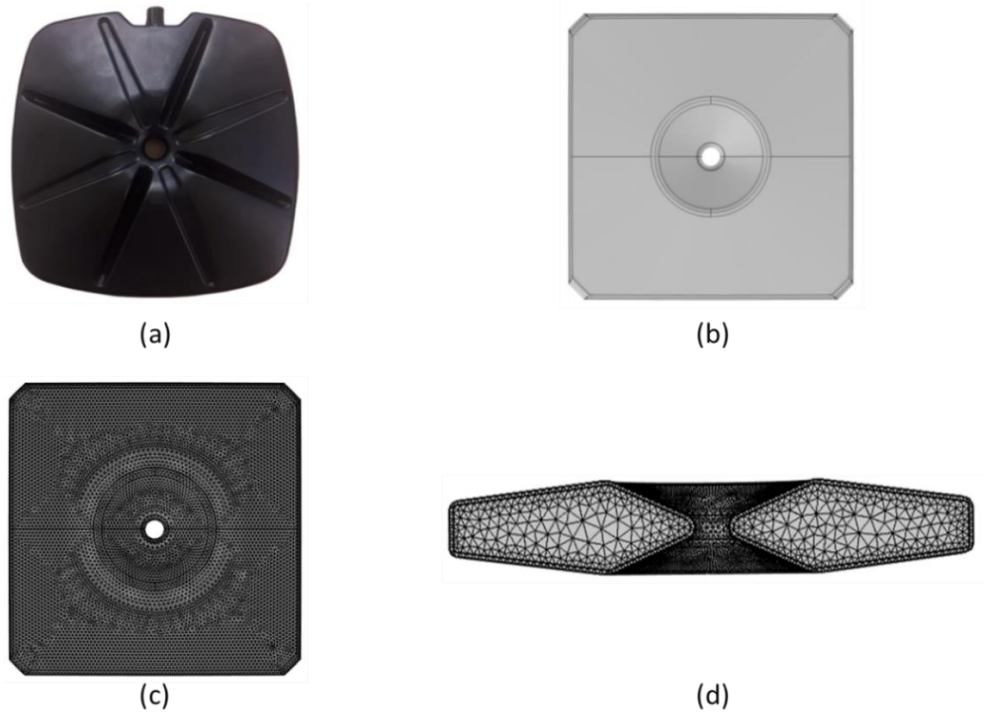

Figure 19 : Illustration of HeatSel; (a) HeatSel capsule, (b) Approximated CAD model, (c) Top view in computational model, and (d) Cross-sectioned view in computational model

3.3. Lab Rig Setup

A lab-scale PumpHeat validation site is constructed at KTH, Sweden for testing LHTES performance. The existing auxiliary setup consists of heating devices (Heat Pump, Electric Heater), tanks (thermal storage tank, Hot and Cold inertia tanks), directional valves and measurement devices (T-Type thermocouples, Resistance Temperature Detectors, flowmeters, and differential pressure transmitter).

During the charging phase, an electric heater (labeled as H in Fig.20) which is controlled by PID supplies the exact amount of heat needed to water (which acts as an HTF), to reach a user-defined temperature point. And the centrifugal pump (P-1) adjusts the speed to deliver water at the required flowrate. While during the discharging phase the heat from the heat storage tank is released in the atmosphere by using a fin-and-coil heat exchanger (labeled as Q, Fig.20). To avoid temperature fluctuations in the HTF, both hot and cold inertia tanks are filled with water at a set temperature. Currently, the heat pump is not in use since the temperature requirement is completed through an electric heater.

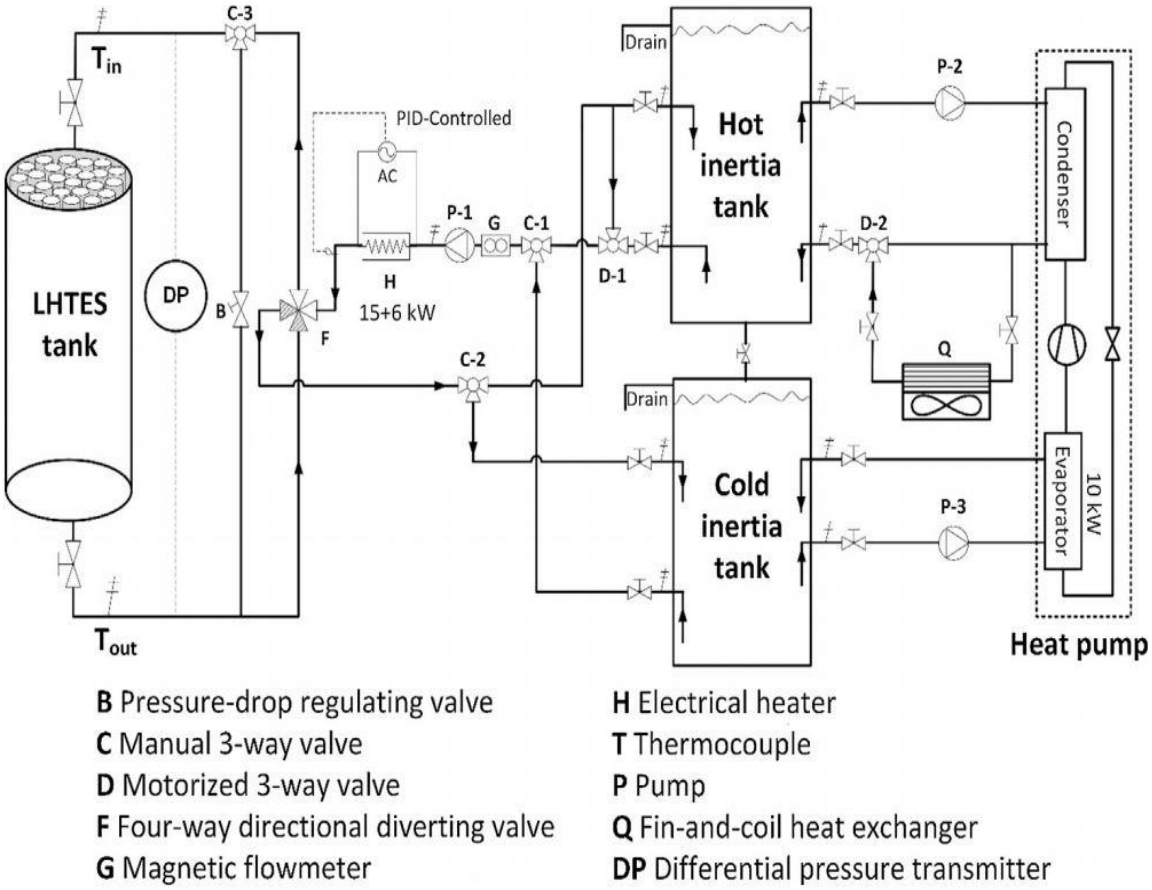

Figure 20 : Schematics of the main existing auxiliary system [24]

The major components of the auxiliary systems[6] which will not be changed are listed in Table 4 All of them are commercially available products.

Table 4 : Components of Auxiliary system [25]

Component	Model	Description
PID-controller Heater	Thermia EK 15 E (15 kW) and Pahlen 6 kW	A two-step heater with 15+6 kW nominal heating capacity
Fin-and-coil heat exchanger	Alfa Laval DGS501CD12H	Nominal cooling capacity of 12 kW
Pump	Grundfos MAGMA3 32-120FN	Maximum head of 18 meters.
Heat pump	Thermia Diplomat Inverter	Nominal heating capacity of 12 kW

[6] Pictures of some of the main auxiliary component is shown in Appendix-5

Most of the auxiliary system remains the same as used previously for testing Macro-Encapsulations in [24]. Only two changes are made; first, the new storage units are installed and second, an additional hydraulic loop is added to accommodate the new storage unit through a three-way directional valve without disturbing that the existing configuration is not disturbed.

Some new characteristics are added to the new loop as shown in the schematic diagram, Figure 21. To control the proportion of water inlet and outlet to the tank, a three-way valve integrated with a temperature-regulating module is installed. Two inlet pipes are also added to accommodate the new submerged heat exchanger design as discussed in section 3.2.1 of this study. A temperature sensor (TC10/TC11) and a pressure-drop regulating valve (B1/B2) is placed on each inlet pipe [25].

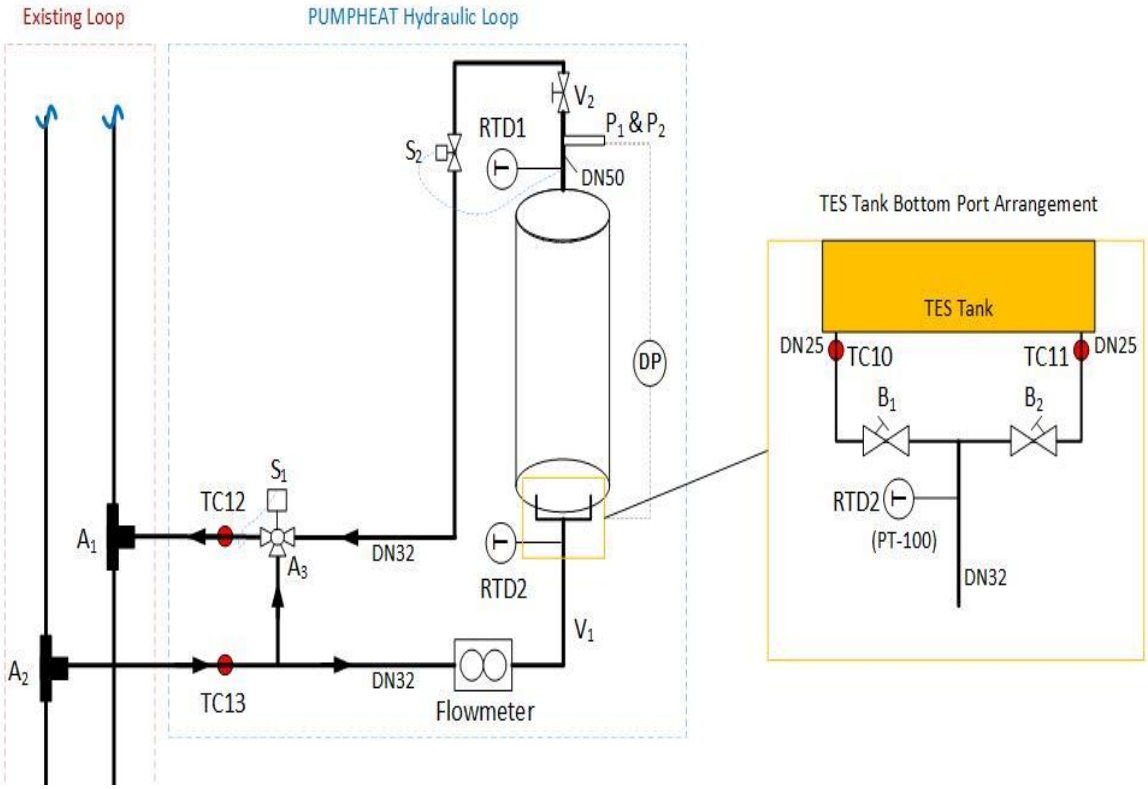

Figure 21 : New hydraulic loop in the existing unit [25]

To measure the flowrate of water, two flowmeters (Yokogawa RXF 032G) are installed; One in the main branch and other in the through the storage unit. The upper limit of the HTF volumetric flowrate range is 5 m^3/h. The analogue signal output is 4-20 mA and the relative accuracy is 0.05% of the measuring span. To have an idea about the flow distribution between two spiral cool loops, two Yokogawa (EJA110A) differential pressure transmitters (DP) are applied in the spiral loops. They have a measurement span of 5-500

kPa and a signal output of 4-20 mA. Pictures of these major auxiliary components are given in the appendix-5.

To measure the temperate throughout the storage tank, eleven T-type thermocouples and nine resistance temperature detectors (PT-100) are installed, labeled as TC and RTD respectively. The location of these temperature sensors can be seen in Figure 22. These temperature sensors were procured from Pentronic AB, already pre-calibrated by the manufacturers. Keithley Data Acquisition and Logging Multimeter System (DAQ6510) along with 40-channel Differential Multiplexer Module plug-in (7708) were purchased to accommodate these temperature sensors.

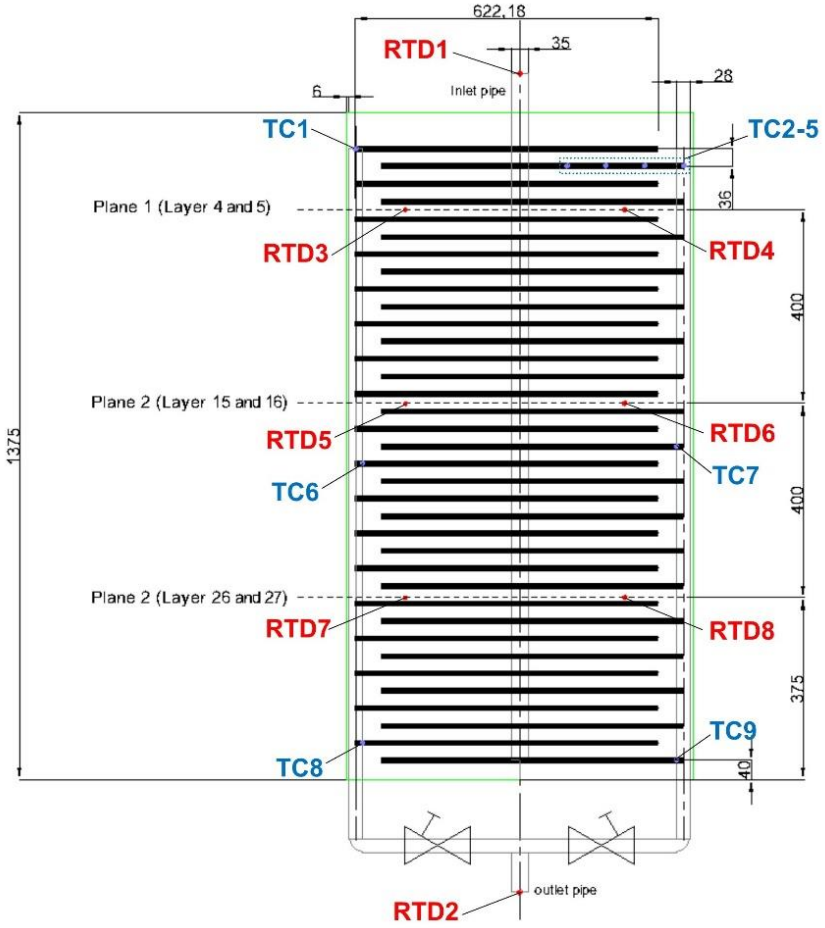

Figure 22: Schematic showing the locations of Temperature sensors [25]

4. Results and Discussions

4.1. Results of Material Selection

The data obtained from the Climate chamber was then filtered and analyzed using VBA (Visual Basic in Applications) in excel sheets. The data was divided into five different heating and cooling cycles. The enthalpy of each test sample is plotted against temperature, Figures 23 and 24, for heat and cooling of the second cycle respectively. The temperature plotted in the x-axis is the average of two thermocouples installed in each sample.

The heating rate is kept as low as 0.1 K/min for both heating and cooling cycles so that the biot number doesn't exceed 0.1 value. After filtering the data by 0.2 the following graphs are plotted for the range of 46 °C to 72°C. For the cooling cycle, the data is not filtered because it will omit the super-cooling phenomenon. All the Enthalpy versus temperature graphs of all the PCM samples is plotted together for the sake of simplicity.

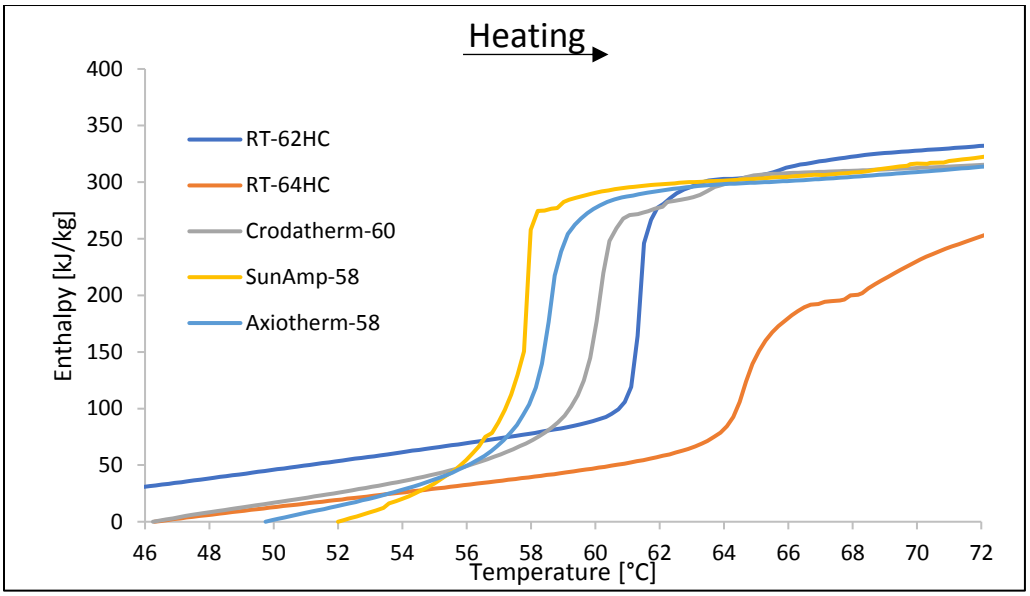

Figure 23 : Charging (Heating) cycle of selected PCM

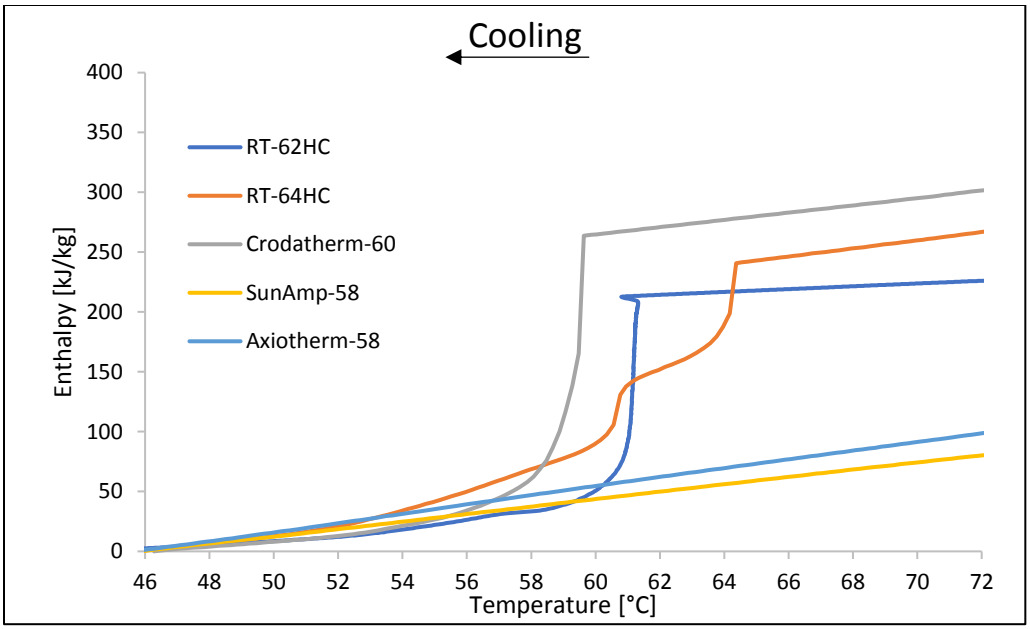

Figure 24 : Discharging (Cooling) cycle of Selected PCM

Instability and uncertainty are seen among the two salt-hydrate PCMs, namely Axiotherm-58 and SunAmp-58. During the second melting cycle, they easily liquify as seen from the enthalpy Figure 23, but during the solidification, both of them don't solidify and the latent enthalpy is also absent Figure 24. This later continues to further cycles where these two samples do not even liquify completely. Furthermore, salt hydrates are also degraded with the passage of time due to phase separation. To avoid this problem these two are discarded. Among the three paraffin samples RT-64HC exhibit two-phase change stages in both heating and cooling cycles as seen in the graphs Figures 23 and 24, one at 64°C and another close to 70°C for heating cycle and for cooling cycle at 60 °C and 64°C, indicating that the material is not pure and is non-homogenous. This will increase the charging/discharging temperature range which is less desirable for LHTES systems. Moreover, 64°C is very high for district water heating applications because it may lead to partial charging and discharging when used in an LHTES. Crodatherm-60 and RT-62HC were the best candidates, Crodatherm-60 had the higher enthalpy change (316 kJ/kg) for a given the temperature range and the heat capacity was noticed to be the highest among the test samples. The specific heat of RT-62HC (227 kJ/kg.K) is slightly higher than Crodatherm-60 (212 kJ/kg.K), probably because of the higher phase temperature, Figure 26. Furthermore, Crodatherm-60 also has the highest thermal conductivity which is considered one of the most important factors considering that fast charging and discharging were required.

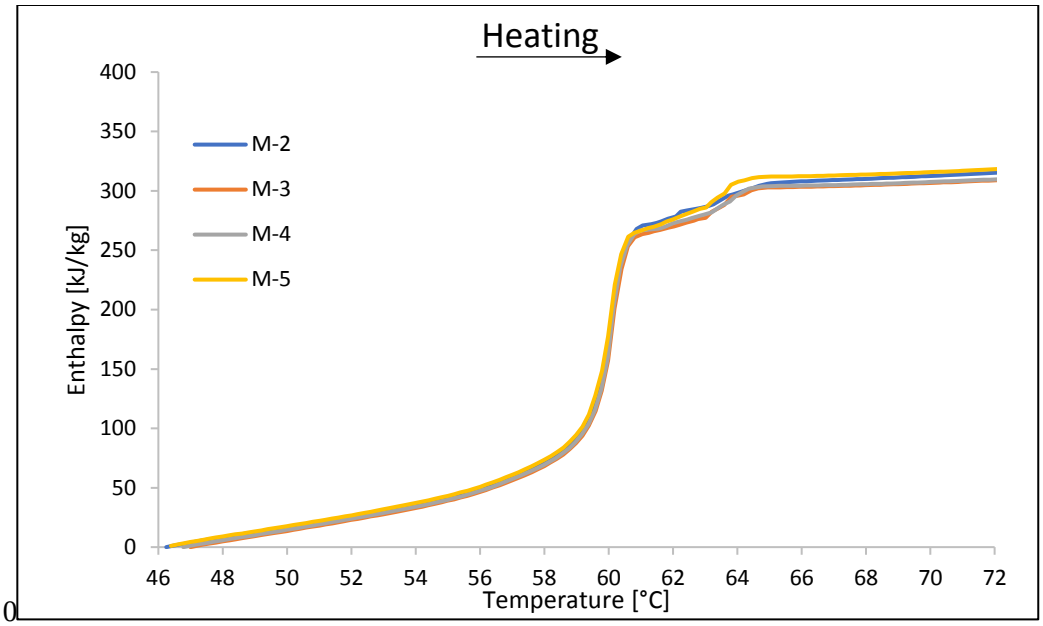

Figure 25: Heating of different cycles of Crodatherm-60

Figure 25 shows the four heating cycles of Crodatherm-60, it can be noticed that there was no uncertainty or instability and almost all the cycles are uniform. Moreover, Crodatherm-60 (5.60 €/kg) was much cheaper than RT-62HC (13 €/kg).

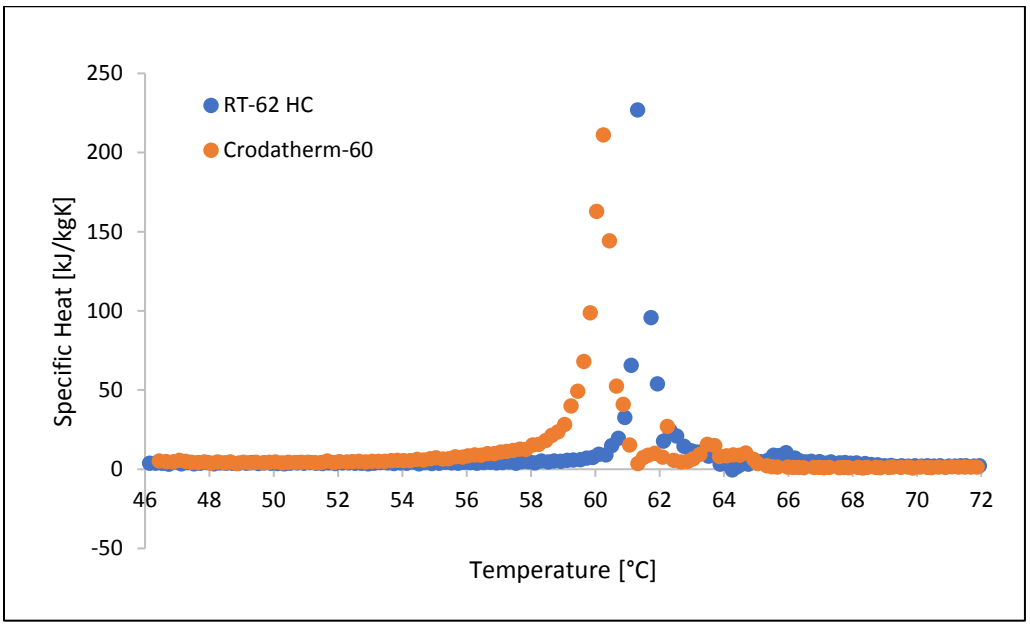

Figure 26 : Specific heat vs. Temperature of RT-62HC and Cordatherm-60

4.2. Result of COMSOL Simulations

The objective of performing the simulation is to check whether the complete PCM inside these encapsulations have a phase change. Moreover, identifying the areas inside the encapsulations where the melting and freezing is difficult to achieve is also part of this study. There are two major criteria is selecting a suitable encapsulation. One is to have a fast charging and discharging process, and the second is to have a complete phase change throughout the PCM volume inside the capsule. For this purpose, the average PCM temperature and the encapsulation are potted against the time, and the cross-sectional view showing the temperature profile is presented in this study.

4.2.1. HeatStixx Result

According to the results obtained from COMSOL, the average PCM temperature (Encapsulation Temp.) reaches the phase change temperature after almost 1000 seconds (16 minutes), hence starting the phase change process, Figure 27. But it is evident from the cross-sectional temperature profile of the model that the temperature is quite low around the axis and the center of the geometry. This area can be seen in Figure 28 (b). Regardless after 7200 seconds (2 hours), the average PCM (PCM Temp.) temperature reaches the final temperature. Moreover, the cross-sectional temperature profile also shows that the temperature even in the hardest areas to melt/freeze region almost reaches 344 K (71°C). It is very safe to say that the phase change takes place throughout the volume of the capsule.

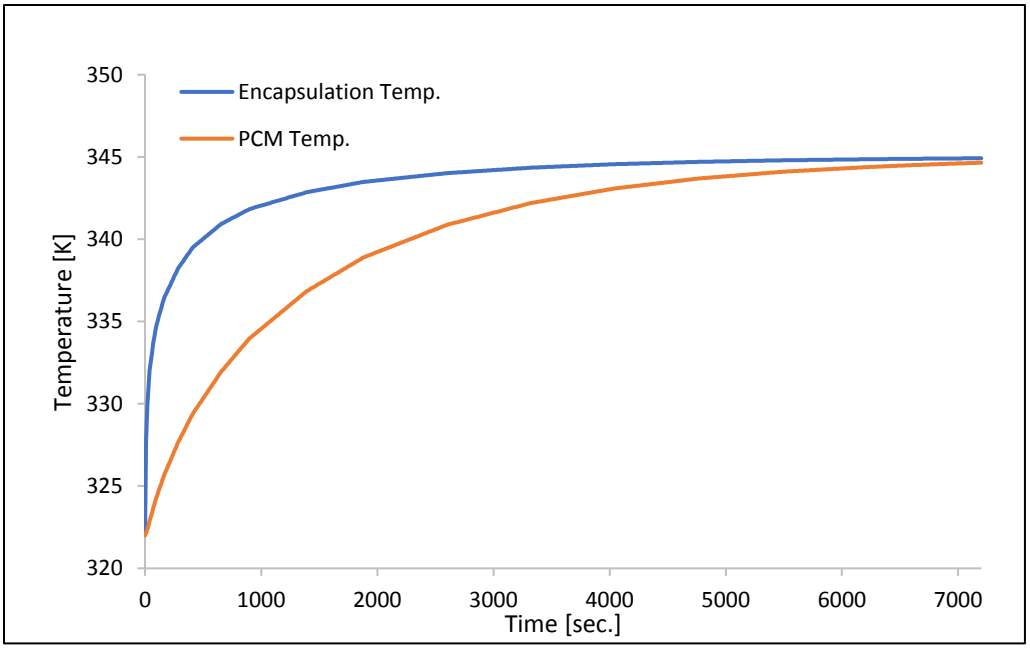

Figure 27 : Temperature vs. Time for HeatStixx

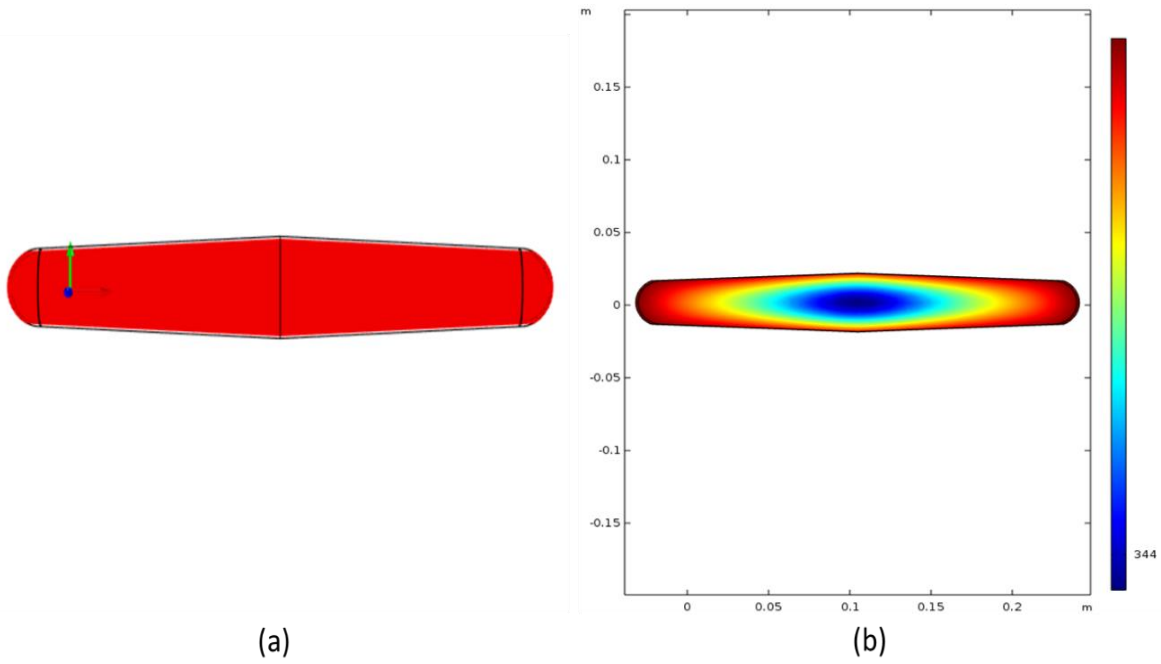

Figure 28 : Results from COMSOL; (a) Cut view of the capsule, (b) Cross-sectional temperature profile

4.2.2. HeatSel Result

The graph presented in Fig.29 shows that the average PCM temperature in the capsule (Encapsulation Temp.) reaches the phase change temperature around 2700 seconds (45 minutes). However, the cross-sectional temperature profile clearly indicates the areas where the temperature difference is much lower, Figure 30 (b). This area is close to the center of the geometry where the thickness of the capsule is also greater. The average PCM temperature (PCM Temp.) reaches 342 K (69°C) after 7200 seconds (2 hours), but the cross-sectional temperature profile indicates some regions where the phase change process just begins at the end of the two hours. The temperature in some regions is as low as 334 K (61°C) because of the capsule thickness in that part, which is highly undesirable. Figure 30 (b) shows the slice in the geometry and the regions which are difficult to melt and solidify during the charging and discharging phase respectively.

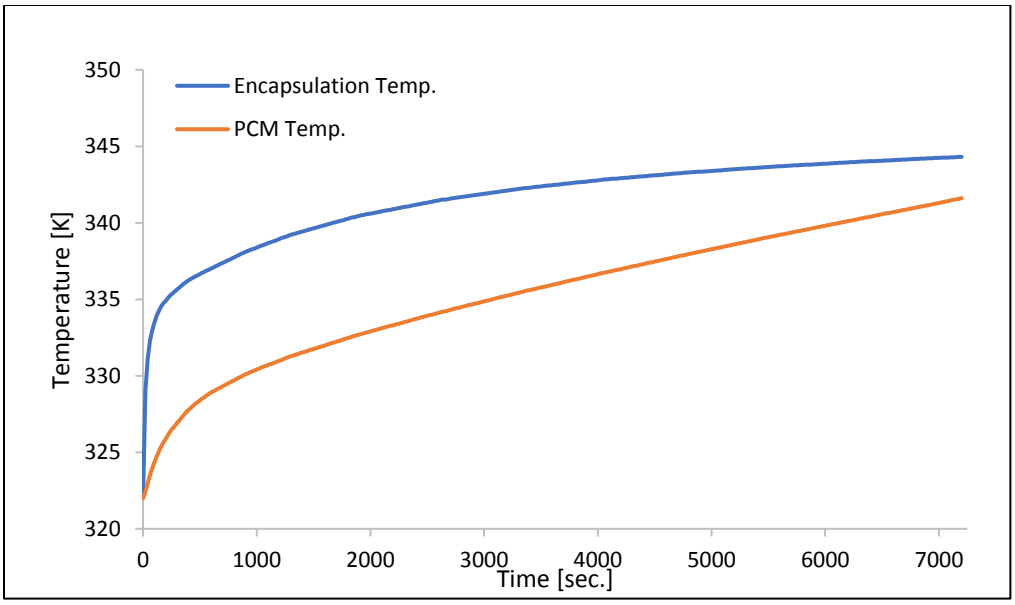

Figure 29 : Temperature vs. Time for HeatSel

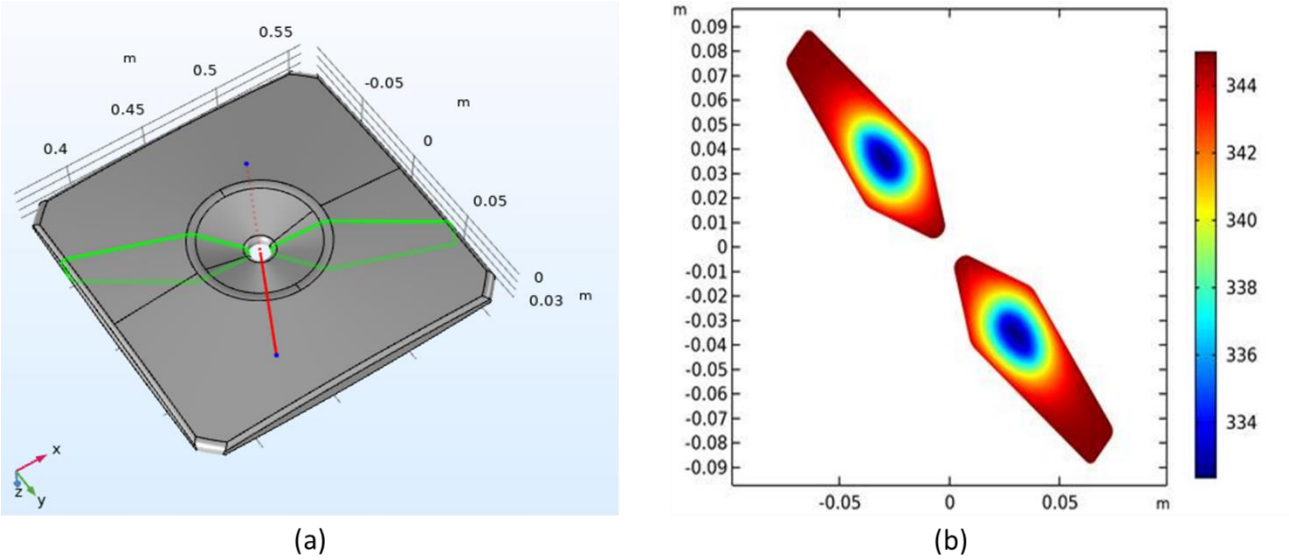

Figure 30 : Results from COMSOL; (a) Cut view of the capsule, (b) Cross-sectional temperature profile

4.3. Total Heat Stored in the Storage Tank

The total amount of heat stored (Latent and Sensible) in the heat exchange can be calculated using the Eq. (1) . The mass of the PCM is calculated by subtracting the volume of the inner structure (Spiral tubes and pipes) with the total volume of the tank for the Submerged Spiral type HX, which is then multiplied by the density of the PCM to get the exact mass.

For the macro-encapsulation ones, the packing factor[7] provided by the supplier is used to calculate the mass of PCM, the packing factor corresponds to the number of capsules which can be placed in per 100 Litres. The total heat stored, and its classification is shown in Table 5. It can be seen from Table 5 that they all have 9 % sensible heat and 91 % latent, this is because of the fact that the same equation was used to calculate for the heat stored over the same temperature range. Since all the types of HXs use same type of energy storage material (Crodatherm-60), they all have the same amount of heat stored per-unit mass. It should be noted here that the only thing distinguishing between these three types of HXs is amount of PCM they can hold for the same volume.

Table 5 :Total amount of Heat Stored

Parameter	**Type of Heat Exchanger**		
	Submerged Spiral type HX	**HeatStixx**	**HeatSel**
Sensible Heat stored (kJ)	12025.69 (9%)	4931.85 (9%)	5240.51 (9%)
Latent Heat stored (kJ)	124594.00 (91%)	51097.20 (91%)	54295.10 (91%)
Total Heat stored (kJ)	136619.70	56029.05	59535.60

[7] Data sheet attached in the Appendix-3

5. Conclusions and Future Work:

After analyzing the results in section 4.2. of this study, it is decided that Crodatherm-60 is the best candidate for this LHTES unit at the given temperature conditions. Crodatherm-60 is thermally very stable and the enthalpy change is also the highest. Furthermore, it is cheaper, non-toxic and non-corrosive nature makes it a perfect candidate for submerged HX.

The spiral submerged HX configuration designed in this study addresses the dead mass PCM problem which was encountered in the previous designs. Moreover, counterflow among different levels and the addition of fins greatly affects the thermal conductivity of the over the system.

Results of the first-ever simulations done on Axiotherm macro-encapsulations in section 4.2., prove that the heatstixx is far better than the HeatSel encapsulations based on the criteria defined earlier. Heatstixx reaches the phase change temperature almost after 16 minutes whereas HeatSel takes almost 45 minutes to reach the same temperature. Furthermore, after the two-hour period, HeatSel will still have PCM which has not undergone a phase change, whilst in HeatStixx the whole volume of PCM undergoes phase change. Even though a price was not the criteria for the selection, it must be noted that HeatStixx is half the price of the HeatSel, and it is also much easier to stack the rods like HeatStixx in the storage tank rather than the slab-like HeatSel.

The submerged spiral type HX can store almost 57 % more heat compared to the HeatStixx and 52 % more compared to the HeatSel. But the spiral HX is known to have a very high charging time whereas, the HeatStixx charge fully charges in almost an hour and HeatSel takes slightly more than two hours. The discharging of all these HXs is much faster. Furthermore, almost 90 % of the total heat stored is Latent heat in all three cases.

The Lab Validation rig is almost ready for preliminary testing, due to time constraints it is not included in this study. Detailed testing of the LHTES system will be done during the next six months. The detailed simulation of spiral type HX can be done to check the effects of decreasing the pitch and counter flow assembly. Moreover, the experimental data received from the experiments can be compared with the simulations to have a better understanding of the approximations which can be taken during the construction of the next LHTES.

Bibliography:

[1] N. ITKONEN, Anna-Kaisa BOCKSTALLER, "Towards a smart, efficient and sustainable heating and cooling sector," *Towards Energy Union: the Commission presents sustainable energy security package*, 2016. [Online]. Available: https://europa.eu/rapid/press-release_MEMO-16-311_it.htm [Accessed: 21-Aug-2019].

[2] I. Sarbu and C. Sebarchievici, "Thermal Energy Storage," in *Solar Heating and Cooling Systems*, Elsevier, 2017, pp. 99–138.

[3] L. F. Mehling, Harald Cabeza, *Heat and cold storage with PCM - An up to date introduction into basics and applications*, First. Berlin: Springer-Verlag Berlin Heidelberg, 2008.

[4] J. Pereira da Cunha and P. Eames, "Thermal energy storage for low and medium temperature applications using phase change materials - A review," *Appl. Energy*, vol. 177, pp. 227–238, 2016.

[5] A. Sharma, V. V. Tyagi, C. R. Chen, and D. Buddhi, "Review on thermal energy storage with phase change materials and applications," *Renew. Sustain. Energy Rev.*, vol. 13, no. 2, pp. 318–345, 2009.

[6] W. S. Andreas Heinz, "Application of Phase Change Materials and PCM slurries for thermal energy storage," in *Ecostock Conference 2006 - Proceeding*, 2006.

[7] L. F. Zalba, B, Marin J, Cabeza, and H. Mehling, "Review on Phase changing materials to store energy," *Appl. Therm. Eng.*, vol. 23, pp. 251–283, 2003.

[8] R. Pilar, L. Svoboda, P. Honcova, and L. Oravova, "Study of magnesium chloride hexahydrate as heat storage material," *Thermochim. Acta*, vol. 546, pp. 81–86, 2012.

[9] H. A. Zondag, R. de Boer, S. F. Smeding, and J. van der Kamp, "Performance analysis of industrial PCM heat storage lab prototype," *J. Energy Storage*, vol. 18, no. October 2017, pp. 402–413, 2018.

[10] M. Medrano, M. O. Yilmaz, M. Nogués, I. Martorell, J. Roca, and L. F. Cabeza, "Experimental evaluation of commercial heat exchangers for use as PCM thermal storage systems," *Appl. Energy*, vol. 86, no. 10, pp. 2047–2055, 2009.

[11] A. López-Navarro *et al.*, "Performance characterization of a PCM storage tank," *Appl. Energy*, vol. 119, pp. 151–162, 2014.

[12] W. Youssef, Y. T. Ge, and S. A. Tassou, "CFD modeling development and experimental validation of a phase change material (PCM) heat exchanger with spiral-wired tubes," *Energy Convers. Manag.*, vol. 157, no. October 2017, pp. 498–510, 2018.

[13] J. N. Chiu (2019), "D3.4 – 'Design and Specifications of Warm Temperature Thermal Storage,'", PumpHeat Internal Report: unpublished.

[14] A. F. Regin, S. C. Solanki, and J. S. Saini, "Heat transfer characteristics of thermal energy storage system using PCM capsules: A review," *Renew. Sustain. Energy Rev.*, vol. 12, no. 9, pp. 2438–2458, 2008.

[15] K. Nithyanandam, J. Stekli, and R. Pitchumani, "High-temperature latent heat storage for

concentrating solar thermal (CST) systems," in *Advances in Concentrating Solar Thermal Research and Technology*, Elsevier, 2017, pp. 213–246.

[16] N. Vitorino, J. C. C. Abrantes, and J. R. Frade, "Quality criteria for phase change materials selection," *Energy Convers. Manag.*, vol. 124, pp. 598–606, 2016.

[17] A. Shukla, K. Kant, and A. Sharma, "Solar still with latent heat energy storage: A review," *Innov. Food Sci. Emerg. Technol.*, vol. 41, pp. 34–46, 2017.

[18] J. N. Chiu (2018), "D3.2 – 'Assessment of Different Options for Thermal Storage in PHCCs,'", PumpHeat Internal Report: unpublished.

[19] J. N. W. Chiu and V. Martin, "Submerged finned heat exchanger latent heat storage design and its experimental verification," *Appl. Energy*, vol. 93, pp. 507–516, 2012.

[20] S. N. Gunasekara, R. Pan, J. N. Chiu, and V. Martin, "Polyols as phase change materials for surplus thermal energy storage," *Appl. Energy*, vol. 162, pp. 1439–1452, 2016.

[21] B. Sandnes and J. Rekstad, "Supercooling salt hydrates: Stored enthalpy as a function of temperature," *Sol. Energy*, vol. 80, no. 5, pp. 616–625, 2006.

[22] T. E. Alam, J. S. Dhau, D. Y. Goswami, and E. Stefanakos, "Macroencapsulation and characterization of phase change materials for latent heat thermal energy storage systems," *Appl. Energy*, vol. 154, pp. 92–101, 2015.

[23] J. T. Wertz, T. C. Mauldin, and D. J. Boday, "Polylactic acid with improved heat deflection temperatures and self-healing properties for durable goods applications," *ACS Appl. Mater. Interfaces*, vol. 6, no. 21, pp. 18511–18516, 2014.

[24] T. Xu, J. N. Chiu, B. Palm, and S. Sawalha, "Experimental investigation on cylindrically macro-encapsulated latent heat storage for space heating applications," *Energy Convers. Manag.*, vol. 182, no. December 2018, pp. 166–177, 2019.

[25] T. Xu, J. N. Chiu (2019), "D3.5 – 'Thermal Storage Prototypes to Demo site and to Validation Sites,'", PumpHeat Internal Report: unpublished.

Appendix-1: Data Sheets of the selected PCMs:

Croatherm-60

CrodaTherm™ 60

High temperature phase change material

CrodaTherm 60 is a water insoluble organic phase change material derived from plant-based feedstocks and has the form of a crystalline wax or oily liquid (depending on temperature).

CrodaTherm 60 is ideal for use in energy storage, electronics, temperature-controlled packaging, automotive and heat recovery applications.

CrodaTherm 60 has a high latent heat capacity, low flammability and is expected to be readily biodegradable.

Typical properties

Thermal properties by *differential scanning calorimetry* (DSC)

Property	Typical Value	Units
Peak melting temperature	59.8 *(139.6)*	°C *(°F)*
Latent heat, melting	217	kJ/kg
Peak crystallisation temperature	58.4 *(137.1)*	°C *(°F)*
Latent heat, crystallisation	-212	kJ/kg

DSC scanning rate: 1°C/ minute

DSC is an analytical technique used for the thermal characterisation of phase change materials. Croda applies the peak melting temperature obtained by DSC in the suffix of the CrodaTherm product name. See appendix for more information on the calorimetry techniques used by Croda

Thermal Properties by *three-layer calorimetry* (3LC*)*

Property	Typical Value	Units
Peak melting temperature	60 *(140)*	°C *(°F)*
Total stored heat, 45°C to 67°C (melting)[1]	215	kJ/kg
Peak crystallisation temperature	60 *(140)*	°C *(°F)*
Total stored heat, 67°C to 45°C (crystallisation)[1]	219	kJ/kg

[1]Heat stored comprises latent heat and sensible heat

3LC is a technique used to assess heat storage properties under conditions that are often closer to those encountered in use. See appendix for more information on the calorimetry techniques used by Croda.

RT-62HC:

Data sheet

RT62HC

RUBITHERM® RT is a pure PCM, this heat storage material utilising the processes of phase change between solid and liquid (melting and congealing) to store and release large quantities of thermal energy at nearly constant temperature. The RUBITHERM® phase change materials (PCM's) provide a very effective means for storing heat and cold, even when limited volumes and low differences in operating temperature are applicable.

We look forward to discussing your particular questions, needs and interests with you.

Properties for RT-line:
- high thermal energy storage capacity
- heat storage and release take place at relatively constant temperatures
- no supercooling effect, chemically inert
- long life product, with stable performance through the phase change cycles
- melting temperature range between -9 °C and 100 °C available

The most important data:

	Typical Values	
Melting area	62-63 main peak: 63	[°C]
Congealing area	62 main peak: 62	[°C]
Heat storage capacity ± 7,5%	230	[kJ/kg]*
Combination of latent and sensible heat in a temperatur range of 55°C to 70°C.	64	[Wh/kg]*
Specific heat capacity	2	[kJ/kg·K]
Density solid at 25 °C	0,85	[kg/l]
Density liquid at 80 °C	0,84	[kg/l]
Heat conductivity (both phases)	0,2	[W/(m·K)]
Volume expansion	2	[%]
Flash point	190	[°C]
Max. operation temperature	90	[°C]

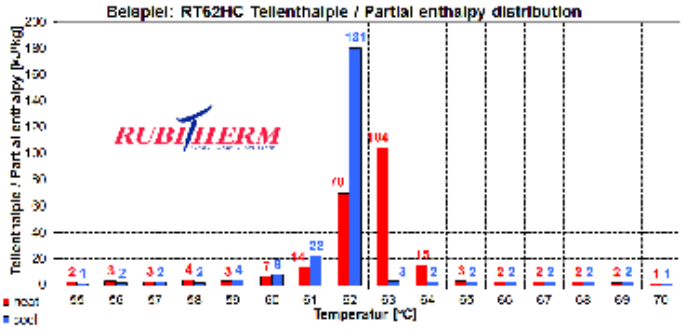

Rubitherm Technologies GmbH
Imhoffweg 6
D-12307 Berlin
Tel: +49 (30) 7109622-0
Fax: +49 (30) 7109622-22
E-Mail: info@rubitherm.com
Internet: www.rubitherm.com

*Measured with 3-layer-calorimeter.

RT-64HC:

Data sheet

RUBITHERM

RT64HC

RUBITHERM® RT is a pure PCM, this heat storage material utilising the processes of phase change between solid and liquid (melting and congealing) to store and release large quantities of thermal energy at nearly constant temperature.
The RUBITHERM® phase change materials (PCM's) provide a very effective means for storing heat and cold, even when limited volumes and low differences in operating temperature are applicable.

We look forward to discussing your particular questions, needs and interests with you.

Properties for RT-line:
- high thermal energy storage capacity
- heat storage and release take place at relatively constant temperatures
- no supercooling effect, chemically inert
- long life product, with stable performance through the phase change cycles
- melting temperature range between -9 °C and 100 °C available

The most important data:

	Typical Values	
Melting area	63-65 main peak: 64	[°C]
Congealing area	64-61 main peak: 64	[°C]
Heat storage capacity ± 7,5% Combination of latent and sensible heat in a temperatur range of 57°C to 72°C.	250 70	[kJ/kg]* [Wh/kg]*
Specific heat capacity	2	[kJ/kg·K]
Density solid at 20 °C	0,88	[kg/l]
Density liquid at 80 °C	0,78	[kg/l]
Heat conductivity (both phases)	0,2	[W/(m·K)]
Volume expansion	11	[%]
Flash point	>190	[°C]
Max. operation temperature	95	[°C]

Beispiel: RT64HC Teilenthalpie / Partial enthalpy distribution

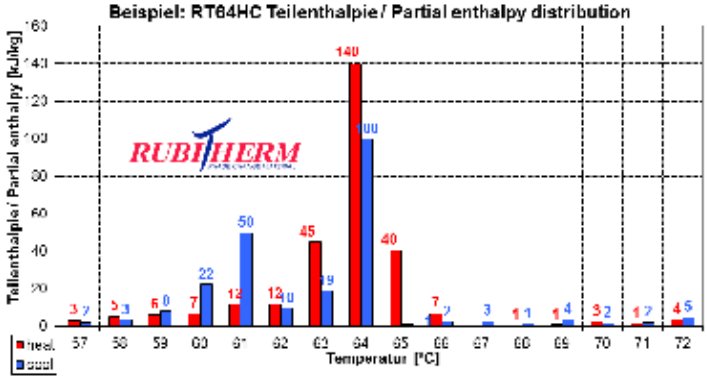

Rubitherm Technologies GmbH
Imhoffweg 6
D-12307 Berlin
Tel: +49 (30) 7109622-0
Fax: +49 (30) 7109622-22
E-Mail: info@rubitherm.com
Internet: www.rubitherm.com

*Measured with 3-layer-calorimeter.

Axiotherm-58:

Data sheet

ATS 58

AXIOTHERM® PCMs are designed to absorb and release large quantities of thermal energy at constant temperatures. Over 30 organic (ATP) and inorganic (ATS) high-performance PCM in a temperature range between -40 °C to 140 ° are available in special macro-encapsulated form with an optimized surface-to-mass ratio for faster energy exchange and improved performance in practical applications. Standardised solutions such as our HeatSel®s and HeatPlates are available for water and air-based applications and can be adapted to your specific requirements.

Key features of the **AXIOTHERM®** PCM are:

- High heat storage capacities
- Consistent, repeatable performance over thousands of thermal cycles
- Simple and safe handling
- Also based on renewable raw materials, nontoxic and biodegradable

		Typical Values
Melting temperature	°C	56 to 58
Congealing temperature	°C	54 to 57
Heat storage capacity* temperature range of 50 – 65°C	kJ/kg	240
Specific heat capacity	kJ/kg*K	3
Density (liquid)	kg/l	1,28
Heat conductivity	W/(m*K)	0,6
Volume expansion	%	>6%
Max. operating temperature	°C	80
Flash point	°C	Non-flammable
Corrosion		Corrosive effect on metalls

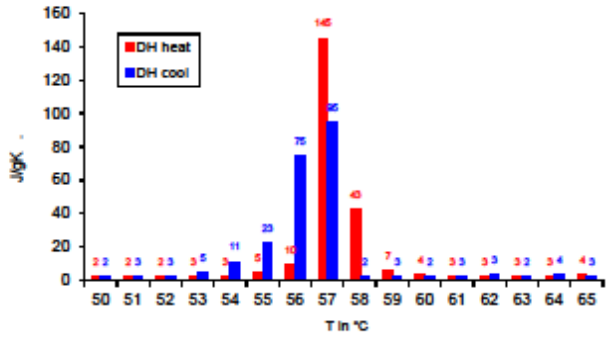

Axiotherm GmbH
Bahnhofstraße 31
D-07607 Eisenberg/Thüringen
Phone: +49 (0) 36691 53 118
Fax: +49 (0) 36691 53 120
E-Mail: Mailbox@axiotherm.de
Web: www.axiotherm.de

*Measured with 3-Layer-Calorimeter

Appendix-2: Blueprints of Storage Tank

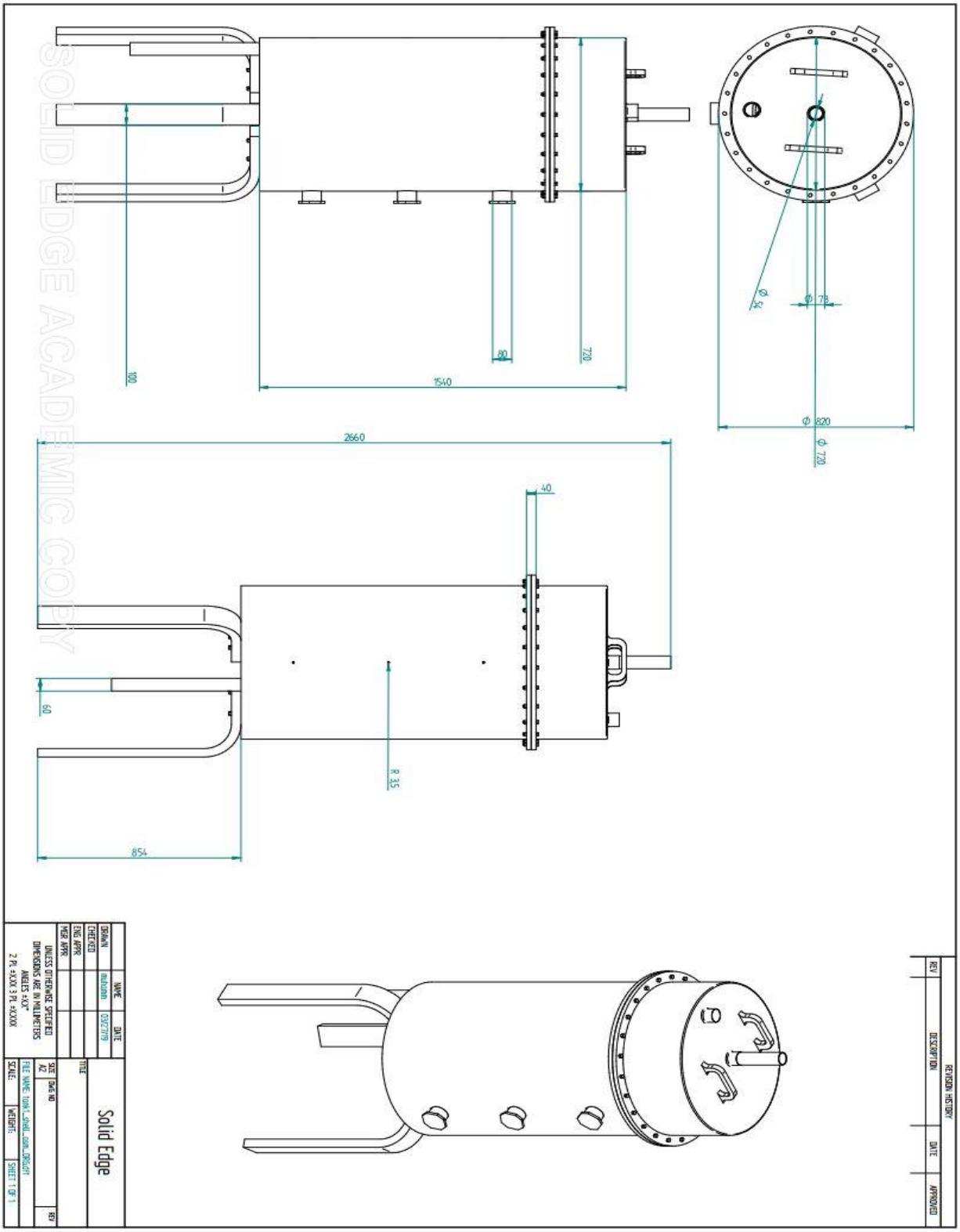

Appendix-3: Axiotherm Storage tank and Macro-Encapsulations

heatStixx	 heatStixx	 heatSel	 heatSel XL
Dimensions	Ø 42 x 310 mm	185 x 185 x 32 mm	275 x 275 x 32 mm
Storage tank size	50 - 1,000 l	500 - 2,000 l	1,500 - 20,000 l
Storage tank diameter	400 - 1,000 mm	600 - 1,200 mm	From 1,200 mm
Number of heatStixx per 100 l storage volume	Approx. 150	Approx. 110	Approx. 37
Installation	1½" sleeve	DN 200 flange	DN 300 flange
Max. operating pressure of storage tank	3 bar	3 bar	3 bar
Pressure loss in the storage tank per m layer thickness	Approx. 20-50 mbar	Approx. 20-50 mbar	Approx. 20-50 mbar
Expansion volume due to phase change	Approx. 5 %	Approx. 5 %	Approx. 5 %
Factor for capacity increase to water (<=0 °C compared to frost protection) at storage tank useful temperature of (varies depending on PCM)	10 K approx. 2.4 to 4.8	10 K approx. 2.5 to 4.9	10 K approx. 2.5 to 4.9
	15 K approx. 2.0 to 3.6	15 K approx. 2.0 to 3.6	15 K approx. 2.0 to 3.6
	30 K approx. 1.5 to 2.4	30 K approx. 1.5 to 2.4	30 K approx. 1.5 to 2.4
Cycle stability	> 10,000 cycles	> 10,000 cycles	> 10,000 cycles

made in germany

It has never been easier to store ecologically generated heat!

Our heatStixx and heatSel are designed such that, in addition to a large surface area, the PCM layer thicknesses are kept so small that the entire PCM participates in the phase change process, thus achieving efficient heat transfer (fast charging and discharging) even with very low temperature differences.

The design as a hybrid heat accumulator enables the greatest possible dynamic due to the water content; it is therefore perfectly suited for a large number of applications in refrigeration, air conditioning and heating technology.

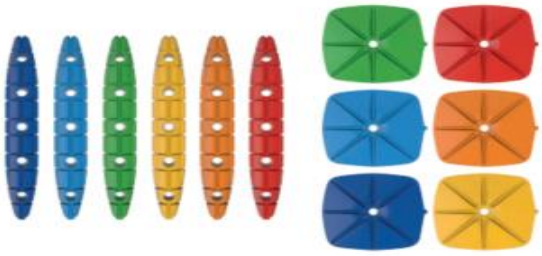

Optimised material properties compared to conventional PCM encapsulations

- Fixed cycle - high phase change resistance (10,000 times)
- Flexible - heatStixx can be adapted to almost any storage system
- Climate neutral - for a better environment and future
- Maintenance-free

➔ Simply select the application temperature, fill with the appropriate heatStixx and immediately use the latent energy.

3

Appendix-4: Blueprints of Spiral copper tube

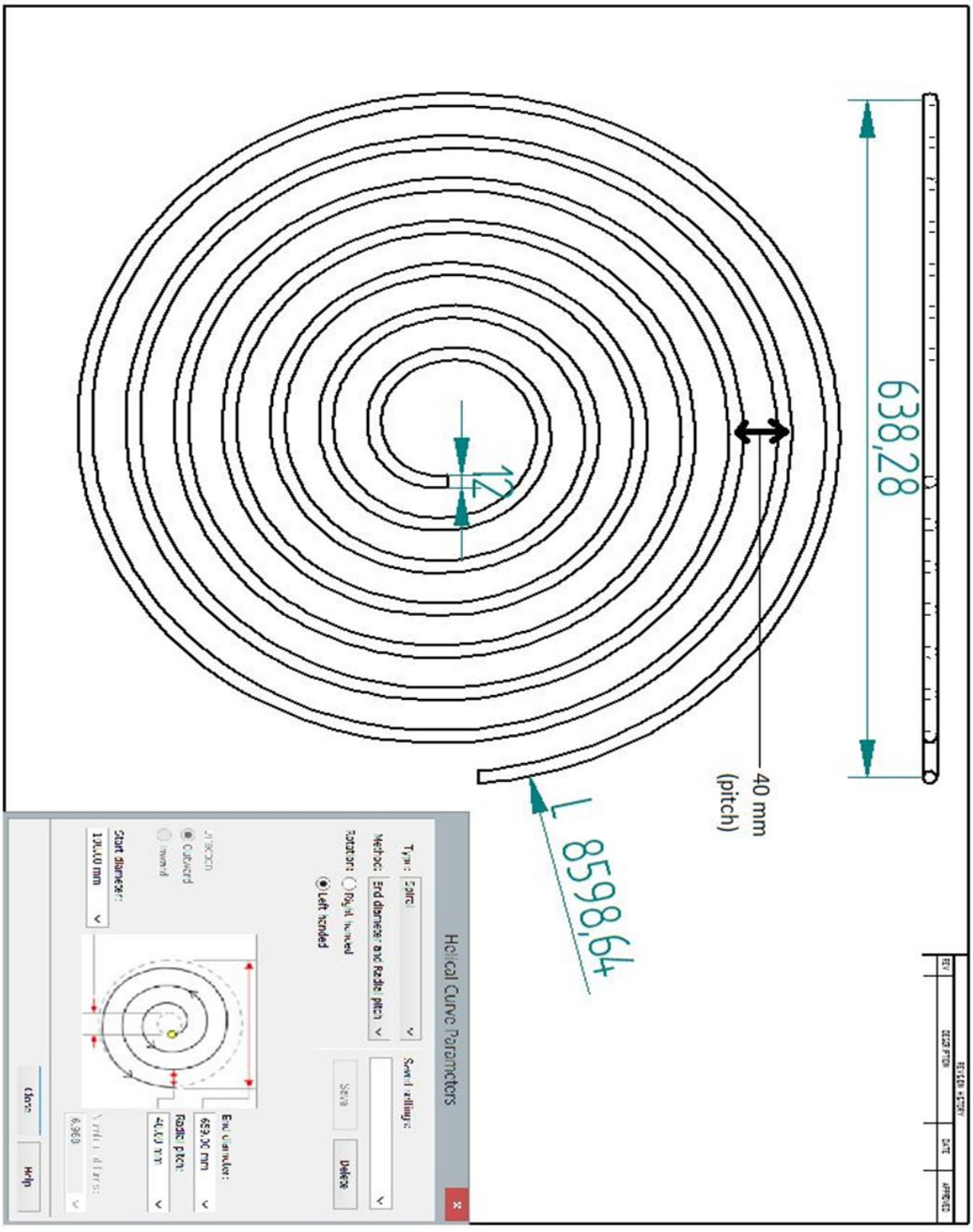

Appendix-5: Pictures of major Auxilary Components.

(a) Storage Tank

(b) Pump

(c) Flowmeter

(d) Differential Pressure Transmitter

(e) HeatPump

(f) Electric Heater